Biomedicine & Pharmacotherapy 175 (2024) 116644

Contents lists available at ScienceDirect

Biomedicine & Pharmacotherapy

journal homepage: www.elsevier.com/locate/biopha

Interplay of OATP1A/1B/2B1 uptake transporters and ABCB1 and ABCG2 efflux transporters in the handling of bilirubin and drugs

Wenlong Li [a,b,*], Rolf W. Sparidans [c], Yaogeng Wang [a], Margarida L.F. Martins [a], Dirk R. de Waart [d], Olaf van Tellingen [a], Ji-Ying Song [e], Maria C. Lebre [a], Stéphanie van Hoppe [a], Els Wagenaar [a], Jos H. Beijnen [a,f,g], Alfred H. Schinkel [a]

[a] The Netherlands Cancer Institute, Division of Pharmacology, Plesmanlaan 121, Amsterdam 1066 CX, the Netherlands
[b] The Second Affiliated Hospital of Nantong University, Shengli Rd 666, Nantong 226001, China
[c] Utrecht University, Faculty of Science, Department of Pharmaceutical Sciences, Division of Pharmacology, Universiteitsweg 99, Utrecht 3584 CG, the Netherlands
[d] Tytgat Institute for Liver and Intestinal Research, Academic Medical Center, Meibergdreef 71, Amsterdam 1105 BK, the Netherlands
[e] The Netherlands Cancer Institute, Division of Experimental Animal Pathology, Plesmanlaan 121, Amsterdam 1066 CX, the Netherlands
[f] Utrecht University, Faculty of Science, Department of Pharmaceutical Sciences, Division of Pharmacoepidemiology & Clinical Pharmacology, Universiteitsweg 99, Utrecht 3584 CG, the Netherlands
[g] The Netherlands Cancer Institute, Department of Pharmacy & Pharmacology, Plesmanlaan 121, Amsterdam 1066 CX, the Netherlands

ARTICLE INFO

Keywords:
Transmembrane drug transporters
Interplay
Novel mouse model
Bilirubin
Plasma exposure
Tissue distribution

ABSTRACT

Transmembrane drug transporters can be important determinants of the pharmacokinetics, efficacy, and safety profiles of drugs. To investigate the potential cooperative and/or counteracting interplay of OATP1A/1B/2B1 uptake transporters and ABCB1 and ABCG2 efflux transporters in physiology and pharmacology, we generated a new mouse model (*Bab12*), deficient for Slco1a/1b, Slco2b1, Abcb1a/1b and Abcg2. *Bab12* mice were viable and fertile. We compared wild-type, *Slco1a/1b/2b1*$^{-/-}$, *Abcb1a/1b;Abcg2*$^{-/-}$ and *Bab12* strains. Endogenous plasma conjugated bilirubin levels ranked as follows: wild-type = *Abcb1a/1b;Abcg2*$^{-/-}$ << *Slco1a/1b/2b1*$^{-/-}$ < *Bab12* mice. Plasma levels of rosuvastatin and fexofenadine were elevated in *Slco1a/1b/2b1*$^{-/-}$ and *Abcb1a/1b;Abcg2*$^{-/-}$ mice compared to wild-type, and dramatically increased in *Bab12* mice. Although systemic exposure of larotrectinib and repotrectinib was substantially increased in the separate multidrug transporter knockout strains, no additive effects were observed in the combination *Bab12* mice. Significantly higher plasma exposure of fluvastatin and pravastatin was only found in Slco1a/1b/2b1-deficient mice. However, noticeable transport by Slco1a/1b/2b1 and Abcb1a/1b and Abcg2 across the BBB was observed for fluvastatin and pravastatin, respectively, by comparing *Bab12* mice with *Abcb1a/1b;Abcg2*$^{-/-}$ or *Slco1a/1b/2b1*$^{-/-}$ mice. Quite varying behavior in plasma exposure of erlotinib and its metabolites was observed among these strains. *Bab12* mice revealed that Abcb1a/1b and/or Abcg2 can contribute to conjugated bilirubin elimination when Slco1a/1b/2b1 are absent. Our results suggest that the interplay of Slco1a/1b/2b1, Abcb1a/1b, and Abcg2 could markedly affect the pharmacokinetics of some, but not all drugs and metabolites. The *Bab12* mouse model will represent a useful tool for optimizing drug development and clinical application, including efficacy and safety.

1. Introduction

Membrane transporters have been identified as important determinants of the transmembrane passage of therapeutic drugs but also endogenous compounds [1,2]. They can be involved in the maintenance of cell homeostasis and implicated in the development and

Abbreviations: ABC, ATP-binding cassette; *Abcb1a/1b;Abcg2*$^{-/-}$, Abcb1a/1b and Abcg2 knockout mice; ANOVA, analysis of variance; AUC, area under plasma concentration-time curve; *Bab12*, mice homozygously deficient for all *Slco1a/1b*, *Slco2b1*, *Abcb1a/1b*, and *Abcg2* genes; BBB, blood-brain barrier; BDG, bilirubin diglucuronide; BMG, bilirubin monoglucuronide; C_{max}, maximum drug concentration in plasma; CYP, Cytochrome P450; LC-MS/MS, liquid chromatography coupled with tandem mass spectrometry; OATP, organic anion-transporting polypeptides; SD, standard deviations; *Slco1a/1b/2b1*$^{-/-}$, Slco1a/1b/2b1 knockout mice; T_{max}, time to reach maximum drug concentration in plasma; UCB, unconjugated bilirubin; Ugt1a1, UDP-glucuronosyltransferase 1a1.

* Correspondence to: Division of Pharmacology, The Netherlands Cancer Institute, Plesmanlaan 121, Amsterdam 1066 CX, the Netherlands
E-mail address: Wenlong.Li@cruk.cam.ac.uk (W. Li).

https://doi.org/10.1016/j.biopha.2024.116644
Received 27 January 2024; Received in revised form 8 April 2024; Accepted 24 April 2024

progression of some diseases [3–5]. Net drug movement can be facilitated or prevented by transmembrane transporters, which can modulate absorption, distribution, and elimination of drugs, thus affecting their pharmacokinetics, and hence the efficacy and safety profiles [1].

Mammalian multispecific drug transporters, typically localized at either the basolateral or apical membrane in polarized cells, belong to two main superfamilies: solute carrier (SLC) transporters and ATP-binding cassette (ABC) transporters, generally mediating cellular influx or efflux of substrates, respectively [6,7]. The SLCO family of drug uptake transporters, namely the organic anion transporting polypeptides 1 A/1B/2B1 (OATP1A/1B/2B1) and the ABC drug efflux transporters MDR1 P-glycoprotein (ABCB1) and breast cancer resistance protein (BCRP; ABCG2) are of profound interest due to their broad substrate specificity and expression in pharmacokinetically important tissues, including excretory organs (liver, intestine, kidney) and critical barrier sites (such as the intestine, placenta and blood-brain barrier) [8–10]. These transporters have also been detected in tumor cells, potentially affecting resistance or susceptibility to anticancer drugs [11,12].

Most of these transporters have substantial overlap in tissue expression and substrate specificities, working in concert to modulate the pharmacokinetic disposition of shared substrates. In addition, together with metabolizing enzymes, the interplay between uptake transporters and efflux transporters may be essential for efficient sequential traverse of the basolateral and apical membrane, so-called 'drug transporter-metabolism interplay' [13,14]. For example, OATP drug uptake transporters may extract their substrates from blood into hepatocytes and enterocytes to get metabolized, then metabolite(s) can be excreted and eliminated by ABC efflux transporters. In this detoxification system, drug uptake transporters deliver the drug to the enzymes to facilitate metabolism, whereas drug efflux transporters relieve the load on enzymes, coordinating to warrant efficient drug elimination [14]. For drugs that are not subject to extensive metabolism *in vivo*, such as fexofenadine [15], the two elements of the 'drug transporter interplay' system may become the main detoxification system by the tandem functions of first uptake and subsequent pumping out of the drug by these transporters.

Variations in activity of drug-metabolizing enzymes, most notably those of the cytochrome P450 (CYP) superfamily, have been extensively investigated to explain the variable behavior of drugs [16,17]. However, there is growing evidence that inter-individual variability in drug pharmacokinetics due to (in part ethnicity-dependent) transporter genetic polymorphisms or transporter-mediated drug-drug interactions is also an important determinant of the efficacy and toxicity of drugs [18–21]. For instance, statins, particularly the pharmacologically active acid forms of statins, have been suggested to be highly dependent on drug transporters for their disposition and efficacy [22,23]. The possible roles of single uptake or efflux transporters in physiology and pharmacology have been assessed in genetically modified cell lines and animal models, as well as (pre-)clinical drug-drug interaction studies [24], but still could not fully explain the variable pharmacokinetic behavior of many drugs. Moreover, it is as yet largely unknown what the potential additional effects of the *in vivo* interplay of these transporters can be.

Importantly, at many pharmacological barrier sites in the body, both efflux and uptake transporters with overlapping substrate specificities are thought to be active at the same time, for instance the intestinal barrier, hepatocyte sinusoidal membrane and biliary canaliculi, and blood-brain barrier (BBB). As the activities of some of these transporters may compensate or even overwhelm the function of the transporters working in the opposite direction, it could sometimes become very hard to directly establish an *in vivo* function for certain transporters with respect to certain drugs. One way to increase the sensitivity of this system is to first knock out transporters with an opposing function, and then test drug behavior in the presence or absence of the transporter of interest. The reduced background transport should make it easier to convincingly establish a transport function for a certain drug by the transporter of interest. We have previously made knockout mouse models deficient for either a number of broad-specificity efflux transporters (Abcb1a/1b/Abcg2), or for a number of broad-specificity uptake transporters (Slco1a/1b/2b1) [25]. As there is substantial overlap in drug substrates between these efflux and uptake transporters, we considered it would be useful to generate and study combination knockout mice for these systems, allowing for more sensitive analyses of transepithelial drug movement.

For that purpose we here generated and characterized a new mouse model lacking the activity of all the Slco1a/1b, Slco2b1, Abcb1a/1b, and Abcg2 transporters. Together with wild-type and appropriate *Slco1a/1b/2b1*$^{-/-}$ and *Abcb1a/1b;Abcg2*$^{-/-}$ strains as controls, we used these models to explore the interplay of the transporters in physiological functions and their *in vivo* pharmacological and toxicological impact using several substrate probes.

2. Materials and methods

2.1. Chemicals and reagents

Rosuvastatin and repotrectinib were supplied by TargetMol (Boston, MA). Fexofenadine, fluvastatin, and erlotinib were purchased from MedChem Express (Monmouth Junction, NJ). Pravastatin was obtained from Sequoia Research Products (Pangbourne, UK). Larotrectinib was purchased from Carbosynth (Oxford, UK). Isoflurane was purchased from Pharmachemie (Haarlem, The Netherlands), and heparin (5000 IU/ml) was from Leo Pharma BV (Breda, The Netherlands). Bovine Serum Albumin (BSA) fraction V was from Roche Diagnostics (Mannheim, Germany). All other chemicals and reagents were obtained from Sigma-Aldrich (Steinheim, Germany).

2.2. Generation of Bab12 mice

Combination knockout (*Bab12*) mice homozygously deficient for all mouse *Slco1a/1b*, *Slco2b1*, *Abcb1a/1b*, and *Abcg2* genes were generated by cross-breeding previously described Slco1a/1b/2b1 knockout (*Slco1a/1b/2b1*$^{-/-}$) mice with Abcb1a/1b and Abcg2 knockout (*Abcb1a/1b;Abcg2*$^{-/-}$) mice.

2.3. Animals

Mouse housing and handling were according to institutional guidelines complying with Dutch and EU legislation. All experimental animal protocols, including power calculations, designed under the nationally approved DEC/CCD project AVD301002016595 were evaluated and approved by the institutional animal care and use committee. Wild-type, *Slco1a/1b*$^{-/-}$, *Slco1a/1b/2b1*$^{-/-}$, *Abcb1a/1b;Abcg2*$^{-/-}$ and *Bab12* mice, all of a >99% FVB genetic background were analyzed [8,25]. The age of the mice was between 58 and 68 weeks for ageing experiments, and between 9 and 16 weeks for the other experiments. The animals were kept in a specific pathogen-free and temperature-controlled environment with a 12-hour light and 12-hour dark cycle and they received a standard medium-fat diet (Transbreed, SDS Diets, Technilab-BMI, Someren, The Netherlands) and acidified water *ad libitum*. Welfare-related assessments were carried out prior to, during, and after the experiments, with mice showing discomfort levels higher than mild being humanely sacrificed.

2.4. Histological analysis

For histopathologic analysis, tissues and organs were fixed in EAF fixative (ethanol/acetic acid/formaldehyde/saline at 40:5:10:45, all v/v) and embedded in paraffin. 2 μm-sections were made from the paraffin blocks and stained with hematoxylin and eosin (H&E) according to standard procedures.

2.5. Sample collection for plasma bilirubin and clinical chemistry analysis and tissue RNA expression levels

Blood was collected by cardiac puncture from wild-type, *Slco1a/1b/2b1*$^{-/-}$, *Abcb1a/1b;Abcg2*$^{-/-}$ and *Bab12* mice in Eppendorf tubes (Hamburg, Germany) containing heparin as an anticoagulant. The mice were sacrificed by cervical dislocation and selected tissues were rapidly collected. The small intestinal contents (SIC) were removed from small intestinal tissue (SI), which was rinsed with cold saline to remove any residual feces. Small pieces (~3 mm^3) of liver, kidney, and SI were collected separately in a 2 ml Eppendorf tube (Hamburg, Germany), and immediately put on dry ice. Plasma was isolated from blood cells by centrifugation at 9000 × *g* for 6 min at 4 °C, then 100 μl was pipetted into brown Eppendorf tubes containing evaporated 1 μl ascorbate (100 mM) by SpeedVac SPD120 Vacuum Concentrator (Thermo Fisher Scientific, Waltham, MA), which was used to prevent oxidation of bilirubin. The remainder of the plasma was used for clinical chemistry measurements. Tissue samples were sent to the Genomics Core Facility in our institute for RNA isolation and RNA sequencing analysis.

2.6. Determination of bilirubin monoglucuronide, bilirubin diglucuronide, and unconjugated bilirubin in plasma

The protocol was adapted from the method described by Spivak and Carey (1985) [26]. In brief, plasma samples were deproteinized with 2 volumes of MeOH after the addition of KOH (final concentration 5 μM). Following centrifugation for 2 min at 14,000 rpm, the supernatant was applied to a Pursuit C18, 5 μm, 3.0 × 100 mm HPLC column (Agilent Technologies, Amstelveen, The Netherlands). Starting eluent consisted of 50% MeOH/50% ammonium acetate (1% (w/v), pH = 4.5) (v/v), followed by a linear gradient to 100% MeOH in 20 min. Detection of bilirubin was performed at 450 nm. Quantification of bilirubin monoglucuronide (BMG), bilirubin diglucuronide (BDG), and unconjugated bilirubin (UCB) was done by using a linear calibration curve of UCB, $1/X^2$ being the weighting factor. Detection limit was 0.05 μM for BMG, BDG, and UCB in plasma.

2.7. Clinical chemistry analysis of plasma

Standard clinical-chemical analyses on heparin plasma were performed on a Roche Hitachi 917 analyzer to determine levels of alkaline phosphatase, aspartate aminotransferase, alanine aminotransferase, γ-glutamyl transferase, lactate dehydrogenase, creatinine, urea, Na^+, K^+, Ca^{2+}, total protein, albumin, uric acid, cholesterol and triglyceride.

2.8. RNA isolation and RNAseq analysis

RNA isolation from male mouse liver, kidney, and small intestine and subsequent RNAseq analysis were performed by the Genomics Core Facility in our institute (Supplemental Data). Equal amounts of the isolated RNAs from the same organ in 6 mice of the same mouse strain were pooled before RNAseq analysis. The expression levels were checked and presented for the following mouse genes: *Slco1a1*, *Slco1a4–6*, *Slco1b2*, *Slco2b1*, *Slc10a1*, *Slc22a1–3*, *Slc22a6–10*, *Slc22a12*, *Abcc2–4*, *Abcb1a*, *Abcb1b*, *Abcg2*, *Aox1*, *Aox3*, *Ugt1a1*, and *Cyp3a*.

2.9. Plasma and tissue pharmacokinetic experiments

Rosuvastatin, fluvastatin, or pravastatin were dissolved in saline at a concentration of 0.5, 1 and 1 mg/ml for oral administration at 5, 10, and 10 mg/kg to mice (10 μl/g), respectively. Fexofenadine was first dissolved in dimethyl sulfoxide (DMSO) at a concentration of 5 mg/ml, followed by 2-fold dilution with polysorbate 80/ethanol (1/1; v/v), and then further diluted with saline to obtain a dose solution of 0.1 mg/ml. Final concentrations of solvents in the dosing solution were: 2%, 1%, 1%, and 96% (all v/v) for DMSO, polysorbate 80, ethanol, and saline, respectively. Larotrectinib was dissolved in DMSO at a concentration of 50 mg/ml and further diluted with 5% glucose in water to yield a concentration of 1 mg/ml. Repotrectinib was dissolved in DMSO at a concentration of 50 mg/ml, which was first diluted 3-fold with ethanol/polysorbate 80 (1/1; v/v), followed by further dilution with a 10 mM hydrochloric acid solution, yielding a dosing solution of 1 mg/ml. The stock solution of erlotinib was prepared in DMSO at 10 mg/ml, and then diluted 100-fold with saline to reach 0.1 mg/ml of dosing solution. All dosing solutions were freshly prepared on the day of experiments.

For pharmacokinetic studies, mice were fasted for 2–3 h to minimize variation in absorption upon oral administration before one of the compounds was administered by gavage into the stomach at 10 μl/g body weight, using a blunt-ended needle. Tail vein serial sampling was performed at indicated time points using heparinized capillary tubes (Sarstedt, Germany). At the last time points, 5 ml pipette tips were used to cover the snout of the mice and they were deeply anesthetized by isoflurane evaporator using 2–3% isoflurane together with 0.2 L/min air and 0.1 L/min oxygen forced flow. Cardiac puncture followed to collect blood in Eppendorf tubes (Hamburg, Germany) containing heparin as an anticoagulant. After sacrificing the anesthetized mice by cervical dislocation, selected tissues were rapidly collected. The small intestinal contents (SIC) were separated from small intestinal tissue (SI), which was rinsed with cold saline to remove any residual feces. Plasma was isolated from blood cells by centrifugation at 9000 × *g* for 6 min at 4°C, and the plasma fraction was collected and stored at −30°C. Tissues were homogenized with appropriate amounts of ice-cold 4% (w/v) bovine serum albumin. All samples were stored at −30°C until analysis.

2.10. LC-MS/MS analysis of drugs and metabolites

The concentrations of rosuvastatin, fexofenadine, fluvastatin, pravastatin [27], larotrectinib [28], repotrectinib [29], erlotinib and its metabolites [30] in plasma samples and tissue homogenates were measured using separate sensitive and specific liquid chromatography-tandem mass spectrometry methods (Supplemental Data).

2.11. Data and statistical analysis

A non-compartmental model using the PKSolver add-in program for Microsoft Excel was adopted to calculate the pharmacokinetic parameters of compounds [31]. Oral availability was assessed by the plasma area under the curve (AUC), calculated using drug plasma concentration-time curves with the linear trapezoidal rule without extrapolating the infinity. Statistical testing was performed in Graphpad Prism7 (Graphpad Software, La Jolla, CA). All data are presented as geometric means ± SD. Heteroscedastic data were log-transformed before applying statistical analysis. One-way analysis of variance (ANOVA) was applied when multiple groups were compared and the Bonferroni *post hoc* correction was used to accommodate multiple testing. Differences were considered statistically significant when $P < 0.05$.

We note here that some data in wild-type, *Slco1a/1b/2b1*$^{-/-}$ and *Abcb1a/1b;Abcg2*$^{-/-}$ mice, presented here for enabling essential direct comparison with the combination *Bab12* mouse data, have been previously reported in a few of our preceding publications [25,32,33]. The main aim of this study was to demonstrate the interplay of transporters using the newly generated combination *Bab12* mice, which requires comparison with the results obtained in the composing "single" knockout strains. Of note, all mouse strains and data collection in this study, when compared, were included in the same experimental setting for each of the studies. Moreover, we have obtained the consent from authors of preceding manuscripts who are not coauthors on this manuscript to include their data in this manuscript. Therefore, all data in this study were appropriately collected and reported according to the journal policy.

3. Results

3.1. Generation and characterization of Slco1a/1b/2b1, Abcb1a/1b, and Abcg2 knockout (Bab12) mice

Combination knockout (*Bab12*) mice homozygously lacking all mouse *Slco1a/1b*, *Slco2b1*, *Abcb1a/1b*, and *Abcg2* genes were generated by cross-breeding previously described Slco1a/1b/2b1 knockout (*Slco1a/1b/2b1*$^{-/-}$) mice with Abcb1a/1b and Abcg2 knockout (*Abcb1a/1b;Abcg2*$^{-/-}$) mice.

Bab12 mice were viable and fertile, although small ageing cohorts showed premature death (before 60 weeks of age) of some *Bab12* mice that was not seen in wild-type mice, suggesting they may have a slightly shortened average life span. Both male and female *Bab12* mice at 9–16 weeks showed significantly higher body weights than wild-type mice (~15–20% increase), but this was also seen in the separate knockout strains, so not a specific phenotype of the combination knockout (Fig. S2). Macro- and microscopic histopathological analysis in young adult *Bab12* mice (12–15 weeks) revealed a few consistent phenotypes in both males and females such as: fatty degeneration of the liver parenchyma; porphyrin-like substances present in the stromal cells of Harderian gland (instead of in the lumen of the acini of the gland), a phenotype previously described also in the single *Abcg2*$^{-/-}$ strain [34]; and active hematopoiesis in the red pulp of spleen accompanied by a hyperplastic lymphoid compartment of the spleen (Fig. S3). Interestingly, these phenotypes of *Bab12* mice became relatively less distinctive compared to wild-type mice when they were aged at around 60 weeks, except for the abnormal porphyrin secretion that remained to the same extent. Furthermore, some age- and FVB strain-related background pathology was encountered in aged male and female *Bab12* mice.

3.2. Expression levels of other transporter proteins in tissues of Abcb1a/1b;Abcg2$^{-/-}$ and Bab12 mice

The expression levels of various uptake and efflux transporters in the liver, kidney, and small intestine of male wild-type, *Slco1a/1b/2b1*$^{-/-}$, *Abcb1a/1b;Abcg2*$^{-/-}$, and *Bab12* mice were determined by RNA sequencing analysis. Hepatic expression of UDP-glucuronosyltransferase 1a1 (*Ugt1a1*) was included, since it catalyzes the glucuronidation of bilirubin and pravastatin. Also, the expression of cytochrome P450 3 A (*Cyp3a*) in the liver and intestine was determined, because it participates in the oxidation of fluvastatin and erlotinib, and possibly of larotrectinib and repotrectinib. The expression levels of these transporters and metabolizing enzymes in wild-type and *Slco1a/1b/2b1*$^{-/-}$ mice have been described before [25]. As shown in Table S1, of all other genes analyzed (other than *Slco1a/1b/2b1*, *Abcb1a/1b*, and *Abcg2*), no major differences in expression were observed in *Abcb1a/1b;Abcg2*$^{-/-}$ and *Bab12* mice compared to wild-type mice in liver and kidney. However, Ugt1a1 RNA in the small intestine of each of the knockout strains was strongly upregulated relative to that in wild-type mice, even to similar levels as normally seen in the liver. This might be related to the higher exposure of certain dietary or endogenous inducing compounds in the knockout mouse strains. Expression of a range of uptake and efflux transporters in mouse brain capillaries was previously analyzed, and found to be unchanged in Abcb1a/1b, Abcg2, and combination ABC transporter knockout mice (Agarwal et al., 2012) [35].

3.3. Analysis of blood and plasma of Abcb1a/1b;Abcg2$^{-/-}$ and Bab12 mice

HPLC-MS/MS analysis of plasma in *Abcb1a/1b;Abcg2*$^{-/-}$ mice, both male and female, demonstrated no significant alterations of endogenous bilirubin levels compared to wild-type mice. We previously demonstrated that all types of bilirubin, including bilirubin mono-glucuronide (BMG), bilirubin di-glucuronide (BDG), and unconjugated bilirubin (UCB), were substantially higher in male *Slco1a/1b/2b1*$^{-/-}$ mice relative to wild-type mice. As shown in Fig. 1A-D and Table S2, in male *Bab12* mice, the BMG and BDG were significantly further increased by 1.25-fold and 1.68-fold, compared to *Slco1a/1b/2b1*$^{-/-}$ mice, respectively. However, the elevated UCB remained unchanged between the two strains. Qualitatively similar results were observed in female mice (Fig. 1E-H). These results suggest that Abcb1a/1b and/or Abcg2 can participate in the disposition of endogenous BMG and BDG, but not UCB, but this contribution can only be observed when Slco1a/1b and Slco2b1 are absent. In addition, the low-density lipoprotein (LDL) cholesterol levels were increased in all the knockout strains compared to the wild-type strain (Tables S3 and S4), which may be associated with the elevated body weight observed in all the knockout strains (Fig. S2). Only in male *Bab12* mice plasma triglycerides were also markedly elevated compared to all other strains. Other measured clinical chemistry parameters were not much altered in *Abcb1a/1b;Abcg2*$^{-/-}$ and *Bab12* mice compared to wild-type mice when considering both genders (Tables S3 and S4).

3.4. Rosuvastatin plasma pharmacokinetics and tissue distribution in Bab12 mice

Rosuvastatin undergoes limited metabolism and is hydrophilic, with very low passive membrane permeability. Its pharmacokinetic disposition is therefore mainly mediated by uptake and efflux transporters [36]. DeGorter et al. (2013) found that nearly 90% of the explainable variability in rosuvastatin plasma levels in patients resulted from two functional transporter polymorphisms, one for the uptake transporter SLCO1B1 and one for the efflux transporter ABCG2 [37]. To assess the combined effects of the Slco1a/1b/2b1 uptake transporters and the Abcb1a/1b and Abcg2 efflux transporters on the oral availability and tissue disposition of rosuvastatin, we performed a 2 h experiment using male wild-type, *Slco1a/1b/2b1*$^{-/-}$, *Abcb1a/1b;Abcg2*$^{-/-}$, and *Bab12* mice, where 5 mg/kg rosuvastatin was orally administered. As shown in Fig. 2A, B and Table S5, rosuvastatin was absorbed very rapidly in wild-type mice, with peak concentrations occurring at or even before 3 min, whereas the T_{max} in all the knockout strains was around 7.5 min. This could mean that these transporters affect the oral absorption phase of rosuvastatin, or that their absence caused delayed elimination of the drug, delaying the T_{max}. Moreover, the plasma AUC_{0-2h} of rosuvastatin was markedly increased by 2.36-fold in *Abcb1a/1b;Abcg2*$^{-/-}$ mice compared to wild-type mice. In *Slco1a/1b/2b1*$^{-/-}$ mice, plasma exposure of rosuvastatin was increased by 24.4-fold, which could be further enhanced by 4.6-fold when Abcb1a/1b and Abcg2 were also deficient, leading to a dramatic increase (112.9-fold) in *Bab12* relative to wild-type mice (Fig. 2C). These results suggest that Slco1a/1b/2b1 and Abcb1a/1b and/or Abcg2 cooperatively limit the oral availability of rosuvastatin.

We observed modestly but significantly reduced brain distribution of rosuvastatin in both Slco1a/1b/2b1-deficient strains (Fig. 2E-F). This is suggestive but not decisive for a possible role of OATPs in the BBB, mediating brain uptake of rosuvastatin: the brain concentrations at this time point in both strains were very low, and the brain-to-plasma ratio differences were mainly driven by the large differences in plasma concentrations. The liver concentrations of rosuvastatin were modestly but significantly increased (1.7–2.1-fold) in the knockout strains (Fig. 2G). After correction for the plasma concentrations, substantially reduced liver-to-plasma ratios of rosuvastatin were found in Slco1a/1b/2b1-deficient mice (21.5-fold), but not in *Abcb1a/1b;Abcg2*$^{-/-}$ mice. Moreover, the rosuvastatin liver-to-plasma ratios were 1.8-fold lower in *Bab12* mice than those in *Slco1a/1b/2b1*$^{-/-}$ mice (Fig. 2H). Liver accumulation of rosuvastatin showed similar shifts (Fig. 2I). These data suggest that liver distribution of rosuvastatin is primarily limited by the uptake transporters Slco1a/1b/2b1, while the Abcb1a/1b and/or Abcg2 efflux transporters could also noticeably contribute to this process, presumably through hepatobiliary excretion, when the Slcos were absent. In addition, the small intestinal content (SIC) levels of rosuvastatin

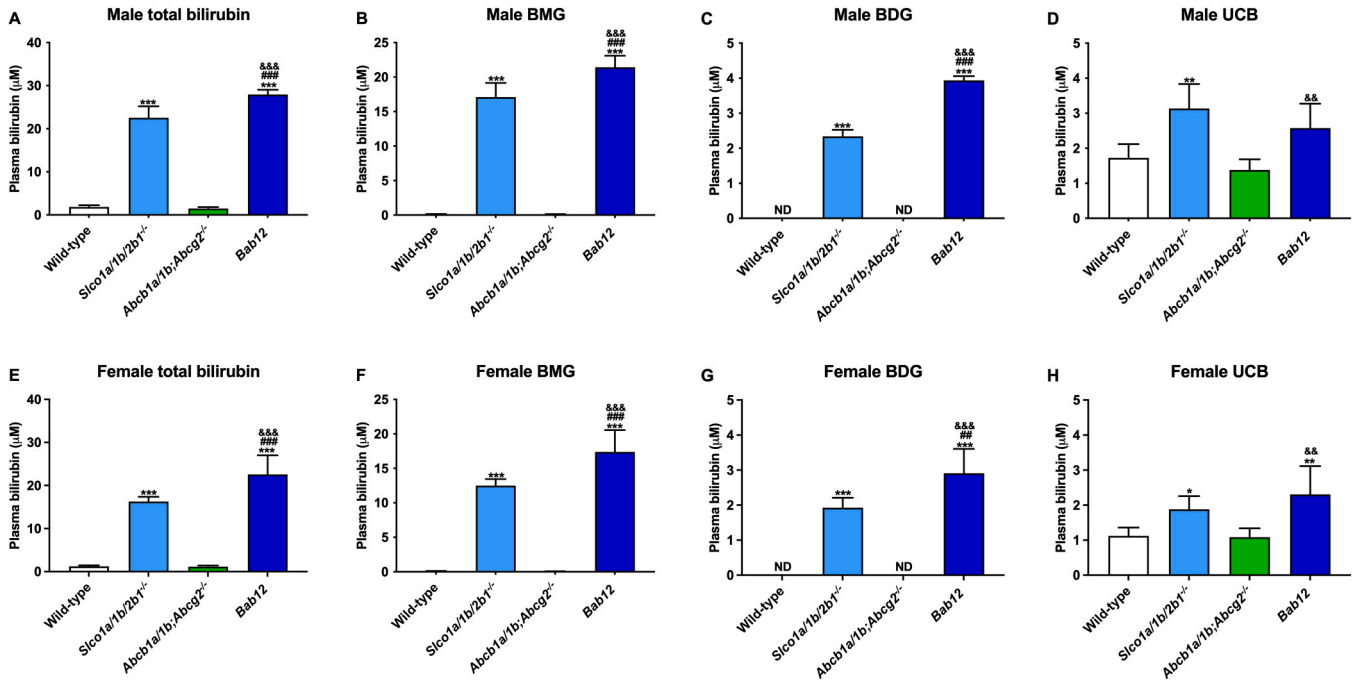

Fig. 1. Endogenous total bilirubin (A, E), bilirubin monoglucuronide, BMG (B, F), bilirubin diglucuronide, BDG (C, G), and unconjugated bilirubin, UCB (D, H) levels in wild-type, *Slco1a/1b/2b1*$^{-/-}$, *Abcb1a/1b;Abcg2*$^{-/-}$, and *Bab12* mice aged 11–13 weeks. Data are presented as mean ± SD (n = 6). *, $P < 0.05$; **, $P < 0.01$; ***, $P < 0.001$ compared to wild-type mice. $^{\#}$, $P < 0.05$; $^{\#\#}$, $P < 0.01$; $^{\#\#\#}$, $P < 0.001$ comparing *Bab12* to *Slco1a/1b/2b1*$^{-/-}$ mice· $^{\&}$, $P < 0.05$; $^{\&\&}$, $P < 0.01$; $^{\&\&\&}$, $P < 0.001$ comparing *Bab12* to *Abcb1a/1b;Abcg2*$^{-/-}$ mice. ND, not detectable; detection limits were 0.05 μM. Note that wild-type and *Slco1a/1b/2b1*$^{-/-}$ data were shown before [25].

were reduced in ABC transporter-deficient mice, but not in *Slco1a/1b/2b1*$^{-/-}$ mice (Fig. 2J-L, Table S5). While the SIC-to-plasma ratios of rosuvastatin were dramatically reduced by 30-fold, 32-fold, and 704-fold in *Slco1a/1b/2b1*$^{-/-}$, *Abcb1a/1b;Acbg2*$^{-/-}$, and *Bab12* mice, respectively. Interestingly, the amount of rosuvastatin recovered in the small intestinal content was around 25% of the total orally administered dose of rosuvastatin in wild-type and *Slco1a/1b/2b1*$^{-/-}$ mice, and this was strongly reduced in *Abcb1a/1b;Abcg2*$^{-/-}$ (1.45%) and *Bab12* (1.65%) mice (Fig. 2J-L). Furthermore, the elimination half-life seemed shorter in both Abcb1a/1b;Abcg2-deficient strains compared to the other two strains, especially from 0.5 to 2 h (Fig. 2B). These results suggest that Abcb1a/1b and/or Abcg2 play an important role in the enterohepatic circulation of rosuvastatin through biliary excretion and/or direct intestinal efflux, resulting in faster and more complete net absorption of rosuvastatin from the SIC in the absence of the ABC transporters. For other tissues we did not observe significant alterations in distribution of rosuvastatin in knockout mice compared to wild-type mice, except for the SI, which followed a similar profile as the SIC (data not shown).

In summary, Slco1a/1b/2b1 mediates hepatic uptake of rosuvastatin, primarily controlling the liver distribution of rosuvastatin. Whereas Abcb1a/1b and/or Abcg2 appear to be heavily involved in the enterohepatic circulation of rosuvastatin, through mediating direct intestinal efflux and/or hepatobiliary excretion. Together, these uptake and efflux transporters can thus dramatically limit the oral availability of rosuvastatin.

3.5. *Fexofenadine plasma pharmacokinetics and tissue distribution in Bab12 mice*

Fexofenadine, a zwitterionic antihistamine, is well absorbed and almost not metabolized upon oral administration in humans, with a bioavailability of 30% [15]. We previously demonstrated that the Slco1a/1b, but not Slco2b1 uptake transporters substantially restrict oral availability of fexofenadine by mediating marked hepatic uptake [25]. Moreover, Tahara et al. (2005) showed that P-glycoprotein (ABCB1) plays an important role in efflux transport in the brain and small intestine but only a limited role in biliary excretion of fexofenadine in mice, affecting plasma concentrations [38]. In addition, considerable variation in fexofenadine pharmacokinetics was observed in human renal transplant recipients, but the cause of most of this variability remained unclear [39]. To investigate the combined roles of these uptake and efflux transporters in plasma exposure and tissue distribution of fexofenadine, 1 mg/kg fexofenadine was orally administered to wild-type, *Slco1a/1b/2b1*$^{-/-}$, *Abcb1a/1b;Abcg2*$^{-/-}$, and *Bab12* mice. Fexofenadine plasma concentrations over 1 h and tissue levels at 1 h were evaluated. As shown in Fig. 3A-C and Table S6, the absorption of fexofenadine was rapid. The plasma AUC_{0-1h} of fexofenadine was markedly increased by 8.5-fold and 4.8-fold in *Slco1a/1b/2b1*$^{-/-}$ and *Abcb1a/1b;Abcg2*$^{-/-}$ mice, respectively, and it was dramatically increased by 52.8-fold in *Bab12* mice, compared to wild-type mice. Of note, in spite of the large inter-strain concentration differences, the plasma concentrations of fexofenadine over time between 15 min and 1 hour remained almost unchanged within each strain, including the Abcb1a/1b;Abcg2-deficient mice (Fig. 3B). This suggests that there was a relatively steady state absorption and elimination of fexofenadine over this period, possibly through a substantial enterohepatic circulation mediated by other transport systems, renal clearance, and/or possibly other (as yet unidentified) processes.

Compared to wild-type mice, the liver-to-plasma ratios were profoundly reduced by around 30-fold in *Slco1a/1b/2b1*$^{-/-}$ and *Bab12* mice, but not in *Abcb1a/1b;Abcg2*$^{-/-}$ mice. A similar shift was observed for fexofenadine liver accumulation (Fig. 3D-F). These data indicate that liver distribution of fexofenadine was strongly affected by Slco1a/1b/2b1. Moreover, the SIC-to-plasma ratio was significantly lower in *Abcb1a/1b;Abcg2*$^{-/-}$ mice than in wild-type mice, and there was a 14.8-fold reduction in SIC-to-plasma ratios in *Bab12* mice compared to *Slco1a/1b/2b1*$^{-/-}$ mice (Fig. 3G-I). These results together suggest that Abcb1a/1b and possibly Abcg2 markedly control intestinal disposition of fexofenadine, mainly through intestinal excretion (effectively reducing the net intestinal uptake of fexofenadine). The lower SIC-to-

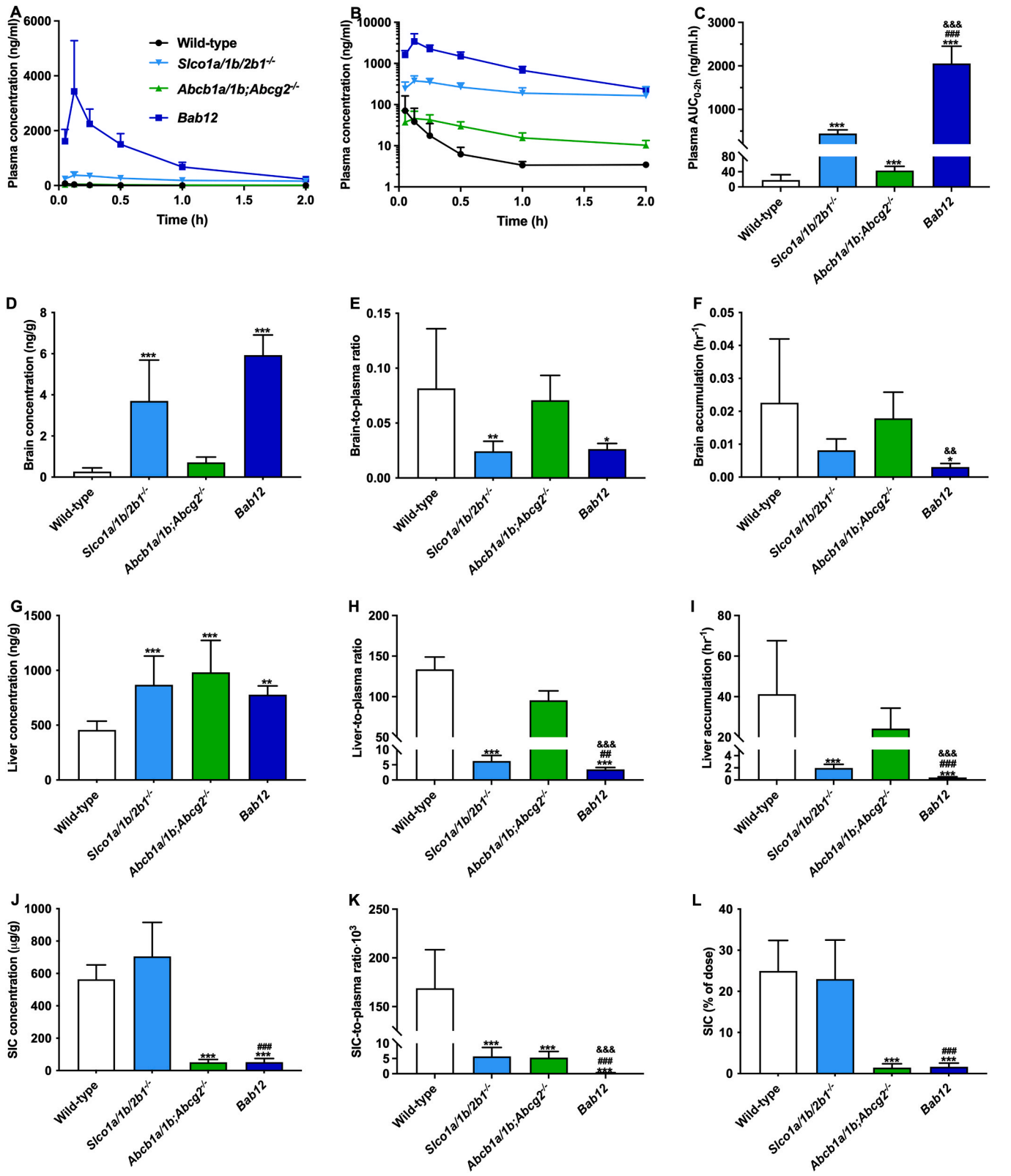

Fig. 2. Rosuvastatin plasma concentration-time curves (A) and semi-log plot of plasma concentration-time curves (B), plasma AUC_{0-2h} (C), brain/liver/SIC concentrations (D, G, J), brain-, liver-, SIC-to-plasma ratios (E, H, K), brain/liver accumulations (F, I), and SIC (% of dose) (L) in male wild-type (n = 6), *Slco1a/1b/2b1*$^{-/-}$ (n = 10), *Abcb1a/1b;Abcg2*$^{-/-}$ (n = 6), and *Bab12* (n = 6) mice after oral administration of 5 mg/kg rosuvastatin. Data are presented as mean ± SD. SIC, small intestinal content. SIC (% of dose), drug percentage of dose in SIC expressed as total rosuvastatin in SIC divided by total drug administered to the mouse. *, $P < 0.05$; **, $P < 0.01$; ***, $P < 0.001$ compared to wild-type mice. $^{\#}$, $P < 0.05$; $^{\#\#}$, $P < 0.01$; $^{\#\#\#}$, $P < 0.001$ comparing *Bab12* to *Slco1a/1b/2b1*$^{-/-}$ mice· $^{\&}$, $P < 0.05$; $^{\&\&}$, $P < 0.01$; $^{\&\&\&}$, $P < 0.001$ comparing *Bab12* to *Abcb1a/1b;Abcg2*$^{-/-}$ mice. Note that wild-type and *Slco1a/1b/2b1*$^{-/-}$ data were presented previously [25].

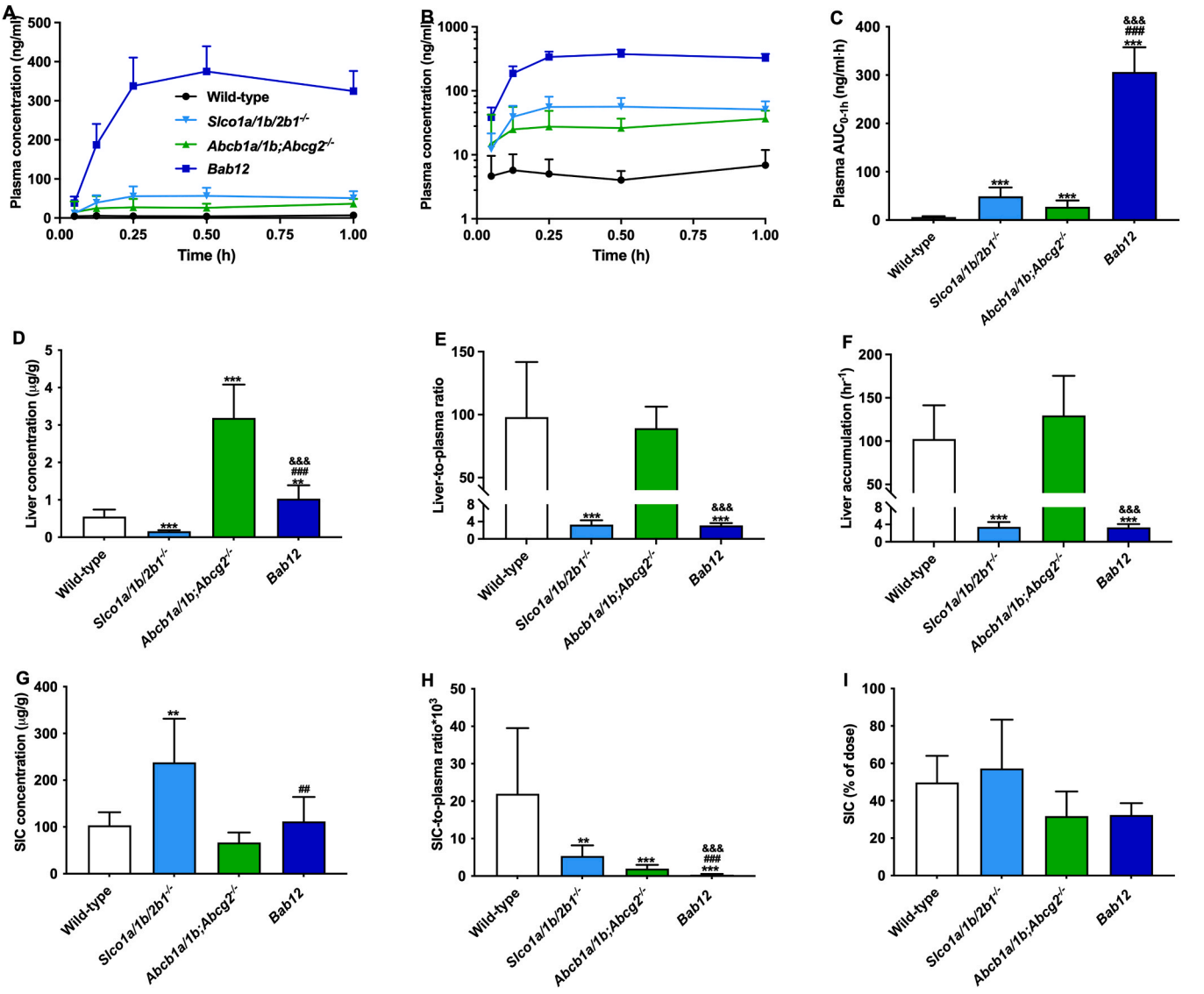

Fig. 3. Fexofenadine plasma concentration-time curves (A) and semi-log plot of plasma concentration-time curves (B), plasma AUC_{0-1h} (C), brain/SIC concentrations (D, G), liver-, SIC-to-plasma ratios (E, H), liver accumulation (F), and SIC (% of dose) (I) in male wild-type, *Slco1a/1b/2b1*$^{-/-}$, *Abcb1a/1b;Abcg2*$^{-/-}$, and *Bab12* mice after oral administration of 1 mg/kg fexofenadine. Data are presented as mean ± SD (n = 6). SIC, small intestinal content. SIC (% of dose), drug percentage of dose in SIC expressed as total fexofenadine in SIC divided by total drug administered to the mouse. *, $P < 0.05$; **, $P < 0.01$; ***, $P < 0.001$ compared to wild-type mice. $^{\#}$, $P < 0.05$; $^{\#\#}$, $P < 0.01$; $^{\#\#\#}$, $P < 0.001$ comparing *Bab12* to *Slco1a/1b/2b1*$^{-/-}$ mice. $^{\&}$, $P < 0.05$; $^{\&\&}$, $P < 0.01$; $^{\&\&\&}$, $P < 0.001$ comparing *Bab12* to *Abcb1a/1b;Abcg2*$^{-/-}$ mice. Wild-type and *Slco1a/1b/2b1*$^{-/-}$ data were presented previously [25].

plasma ratios found in Slco1a/1b/2b1-deficient mice were most likely due to reduced hepatobiliary excretion as a secondary consequence of decreased hepatic uptake. However, no significant alteration in SIC (% of dose) in knockout mice relative to wild-type mice was observed, although both ABC transporter-deficient strains tended towards lower SIC values. This might primarily be due to a large amount of unabsorbed fexofenadine (~30–55%) still resident in the small intestinal content, presumably as a consequence of sluggish intestinal absorption of fexofenadine. Unfortunately, no reliable data about brain distribution of fexofenadine could be obtained as its brain concentrations were below the lower limit of quantification.

Thus, systemic exposure of fexofenadine was limited by the cooperation of Slco1a/1b and Abcb1a/1b, which can facilitate or mediate hepatic uptake and intestinal excretion of fexofenadine, respectively.

3.6. *Fluvastatin plasma pharmacokinetics and tissue distribution in Bab12 mice*

Fluvastatin has been identified as a substrate of human BCRP (ABCG2), OATP1B1, OATP1B3, OATP1A2, and OATP2B1. We previously observed significantly higher oral availability of fluvastatin in *Slco1a/1b*$^{-/-}$ and *Slco1a/1b/2b1*$^{-/-}$ mice [25]. However, Karibe et al. (2015) did not find any changes in plasma exposure of fluvastatin in Abcg2 knockout mice or ABCG2 inhibitor-treated monkeys after oral administration of fluvastatin [40]. In order to assess whether we could observe some additional effects of Slco1a/1b/2b1, Abcb1a/1b, and especially Abcg2 on fluvastatin systemic exposure, we performed a 2 h experiment using male mice from the same four mouse strains described above. As shown in Fig. 4A-C and Table S7, after oral administration of 10 mg/kg of fluvastatin, the plasma concentrations of fluvastatin over 2 h were markedly increased, with significant 10.2-fold and 7.96-fold increases of the plasma AUC_{0-2h} in *Slco1a/1b/2b1*$^{-/-}$ and *Bab12* mice, respectively, compared to wild-type mice, but not in *Abcb1a/1b;Abcg2*$^{-/-}$

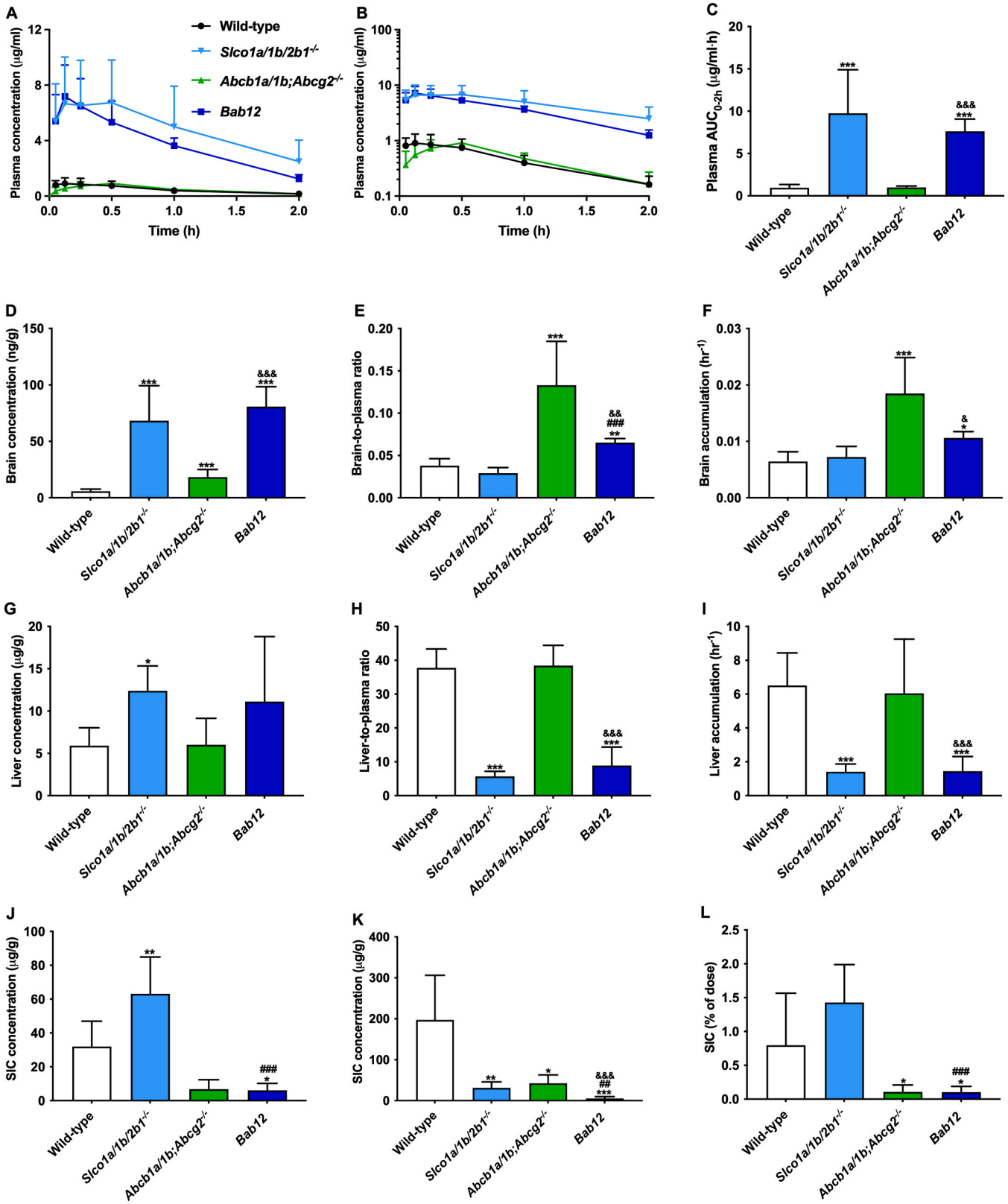

Fig. 4. Fluvastatin plasma concentration-time curves (A) and semi-log plot of plasma concentration-time curves (B), plasma AUC_{0-2h} (C), brain/liver/SIC concentrations (D, G, J), brain-, liver-, SIC-to-plasma ratios (E, H, K), brain/liver accumulations (F, I), and SIC (% of dose) (L) in male wild-type (n = 6), *Slco1a/1b/2b1*$^{-/-}$ (n = 6), *Abcb1a/1b;Abcg2*$^{-/-}$ (n = 4), and *Bab12* (n = 6) mice after oral administration of 10 mg/kg fluvastatin. Data are presented as mean ± SD. SIC, small intestinal content. SIC (% of dose), drug percentage of dose in SIC expressed as total fluvastatin in SIC divided by total drug administered to the mouse. *, $P < 0.05$; **, $P < 0.01$; ***, $P < 0.001$ compared to wild-type mice. $^{\#}$, $P < 0.05$; $^{\#\#}$, $P < 0.01$; $^{\#\#\#}$, $P < 0.001$ comparing *Bab12* to *Slco1a/1b/2b1*$^{-/-}$ mice. $^{\&}$, $P < 0.05$; $^{\&\&}$, $P < 0.01$; $^{\&\&\&}$, $P < 0.001$ comparing *Bab12* to *Abcb1a/1b;Abcg2*$^{-/-}$ mice. Wild-type and *Slco1a/1b/2b1*$^{-/-}$ data were presented previously [25].

mice. The elimination half-lives in all strains from 0.5 h onwards were roughly similar (Fig. 4B). These results indicate that Slco1a/1b/2b1 could profoundly limit the oral availability of fluvastatin, but that Abcb1a/1b and Abcg2 play little, if any, role in this process.

As shown in Fig. 4G-I, the Slco1a/1b/2b1 transporters play primary roles in controlling liver distribution of fluvastatin by mediating hepatic uptake, while Abcb1a/1b and/or Abcg2 control SIC disposition, presumably through intestinal and/or biliary excretion (Fig. 4J-L). Interestingly, we observed substantially elevated brain-to-plasma ratios and brain accumulation of fluvastatin in *Abcb1a/1b;Abcg2*$^{-/-}$ mice. Moreover, the brain-to-plasma ratios of fluvastatin were also significantly (2.2-fold) higher in *Bab12* mice than in *Slco1a/1b/2b1*$^{-/-}$ mice (Fig. 4D-F). These results together demonstrate that Abcb1a/1b and/or Abcg2 could markedly restrict fluvastatin penetration into the brain. It is worth mentioning that the brain-to-plasma ratio and brain accumulation of fluvastatin were markedly decreased in *Bab12* mice compared to *Abcb1a/1b;Abcg2*$^{-/-}$ mice. In contrast, no significant differences were seen between wild-type and *Slco1a/1b/2b1*$^{-/-}$ mice (Fig. 4D-F). These data suggest that Slco1a/1b/2b1 could perhaps mediate uptake of fluvastatin across the BBB into the brain, but this could only be seen when Abcb1a/1b and Abcg2 were absent. It should be noted, though, that the large differences in fluvastatin plasma AUC and concentration between *Bab12* and *Abcb1a/1b;Abcg2*$^{-/-}$ mice may complicate interpretation of these ratios.

3.7. Pravastatin plasma pharmacokinetics and tissue distribution in Bab12 mice

We previously demonstrated that pravastatin is an *in vivo* substrate of both Slco1a/1b and Slco2b1 [25]. We therefore wanted to further explore the effects of Slco1a/1b/2b1, Abcb1a/1b, and Abcg2 on plasma exposure and tissue distribution, especially for brain, of pravastatin. An experiment was carried out up to 2 h using male mice from the same four wild-type and knockout strains, in which 10 mg/kg pravastatin was orally administered. As shown in Fig. 5 and Table S8, the plasma and tissue pharmacokinetics were not much altered between wild-type and *Abcb1a/1b;Abcg2*$^{-/-}$ mice. In contrast, the plasma AUC_{0-2h} was substantially increased by 73.5-fold and 68.6-fold in *Slco1a/1b/2b1*$^{-/-}$ and *Bab12* mice compared to wild-type mice, respectively (Fig. 5A-C). Furthermore, markedly lower liver-to-plasma ratios and SIC-to-plasma ratios were observed in *Slco1a/1b/2b1*$^{-/-}$ and *Bab12* mice, but not in *Abcb1a/1b;Abcg2*$^{-/-}$ mice, relative to those in wild-type mice (Fig. 5G-K). These parameters were also not significantly different between *Slco1a/1b/2b1*$^{-/-}$ and *Bab12* mice. However, we did observe significantly elevated brain-to-plasma ratios (2.2-fold) and brain accumulation (2.0-fold) in *Bab12* mice compared to *Slco1a/1b/2b1*$^{-/-}$ mice, even while the plasma exposure between these strains was very similar. These results indicate that Slco1a/1b/2b1 uptake transporters are important determinants for the systemic, brain, liver and small intestine exposure of pravastatin. Moreover, Abcb1a/1b and/or Abcg2 could modestly limit the brain distribution of pravastatin when the Slco1a/1b/2b1 transporters were absent. Nonetheless, as seen above with fluvastatin, the vast differences in pravastatin plasma exposure and concentration between Slco1a/1b/2b1-proficient and -deficient strains precluded a straightforward detailed interpretation of tissue-to-plasma ratios between these strains.

3.8. Larotrectinib and repotrectinib plasma and tissue pharmacokinetics in Bab12 mice

We previously showed using knockout mice that larotrectinib and repotrectinib are shared *in vivo* substrates of Slco1a/1b uptake transporters and Abcb1a/1b and Abcg2 efflux transporters [32,33]. To assess the possible additional effects and interplay of these transporters *in vivo*, we orally administered larotrectinib or repotrectinib (both at 10 mg/kg) to the same four mouse strains as mentioned above. The plasma exposure (Fig. 6A-C), liver distribution (Fig. 6G-I) and small intestinal tissue accumulation (Fig. 6J-L) of larotrectinib behaved similarly between *Slco1a/1b/2b1*$^{-/-}$ and *Bab12* mice, while they were significantly different from wild-type mice. However, Slco1a/1b/2b1 appeared to have a slightly higher impact on the liver distribution, and Abcb1 and Abcg2 on the intestinal distribution of larotrectinib. In contrast, larotrectinib brain accumulation was only markedly affected by the deficiency of Abcb1a/1b and Abcg2 (Fig. 6D-F). We did not observe any other significant additional impact and interplay of the Slco1a/1b/2b1, Abcb1 and Abcg2 transporters with respect to the plasma and tissue pharmacokinetics of larotrectinib in *Bab12* mice over the time span analyzed (Fig. 6). Qualitatively similar results were observed for repotrectinib pharmacokinetics (Fig. 7A-L), albeit with perhaps a slightly more pronounced impact of the ABC transporters on brain distribution (Fig. 7D-F). Although in this case not *Slco1a/1b/2b1*$^{-/-}$ but *Slco1a/1b*$^{-/-}$ mice were tested because of transient breeding problems with the first strain, the results do not suggest a marked additional effect of Oatp2b1 in this context. Taken together, larotrectinib and repotrectinib plasma exposure and tissue distribution were markedly affected by both uptake transporters and efflux transporters, but their respective effects were not markedly altered by deficiencies in the “opposite” or “complementary” (uptake *vs* efflux) transporters.

3.9. Plasma exposure of erlotinib and its metabolites in Bab12 mice

Our group recently developed and validated an LC-MS/MS method to quantify and semi-quantify the plasma levels of erlotinib and its metabolites, respectively [30]. We applied this to determine the plasma and tissue concentrations in a 4 h pharmacokinetic experiment using the same set of four male mouse strains, after 1 mg/kg erlotinib was orally administered. There were no significant differences in plasma exposure of erlotinib among the different mouse strains (Fig. 8A). Because the plasma metabolite levels (Fig. 8B-F), except for OSI-420, were semi-quantified, we also plotted the metabolite-to-erlotinib ratios in plasma (Fig. 9). This is more relevant to assess the impact of transporters on plasma levels of metabolites, also considering that erlotinib plasma levels were not very different between the strains (Fig. 8A). As shown in Figs. 8 and 9, we observed quite divergent behaviors in plasma exposure of these compounds between the mouse strains. Plasma concentrations and exposure of erlotinib and OSI-420 were not much altered in knockout compared to wild-type strains, although, based on the ratios, elimination of OSI-420 was possibly somewhat delayed in ABC-transporter-deficient mice (Fig. 9A). Significantly higher metabolite-to-erlotinib ratios of OSI-413 and M16 (ring-oxidation) over 4 hours were found in *Abcb1a/1b;Abcg2*$^{-/-}$ mice, but not in *Slco1a/1b/2b1*$^{-/-}$ mice, compared to wild-type mice. And M16, but not OSI-413, showed further increased ratios in *Bab12* relative to *Abcb1a/1b;Abcg2*$^{-/-}$ mice (Fig. 9B, C). In addition, ratios of the other two detectable metabolites (possibly M19 (phenylacetylene oxidation to acetophenone and ring-oxidation) or M6 (phenylacetylene oxidation to carboxylic acid)) and M20 (M16-glucuronide), all based on the transition and retention times) were markedly increased in *Slco1a/1b/2b1*$^{-/-}$ and *Abcb1a/1b;Abcg2*$^{-/-}$ compared to wild-type mice, and were further substantially elevated in *Bab12* mice (Fig. 9D, E). These data suggest that both M19/M6 and M20 were significantly cleared through both the ABC and SLCO transporter systems.

Thus, collectively, the interplay and potential additional effects of the Slco1a/1b/2b1, Abcb1a/1b, and Abcg2 transporters could substantially affect the plasma exposure of some of the erlotinib metabolites, even when they had limited impact on their parental drug.

4. Discussion

By cross-breeding we generated a new mouse model (*Bab12*), deficient for the mouse *Slco1a/1b*, *Slco2b1*, *Abcb1a/1b*, and *Abcg2* genes, to assess the interplay and combined physiological, pharmacological and

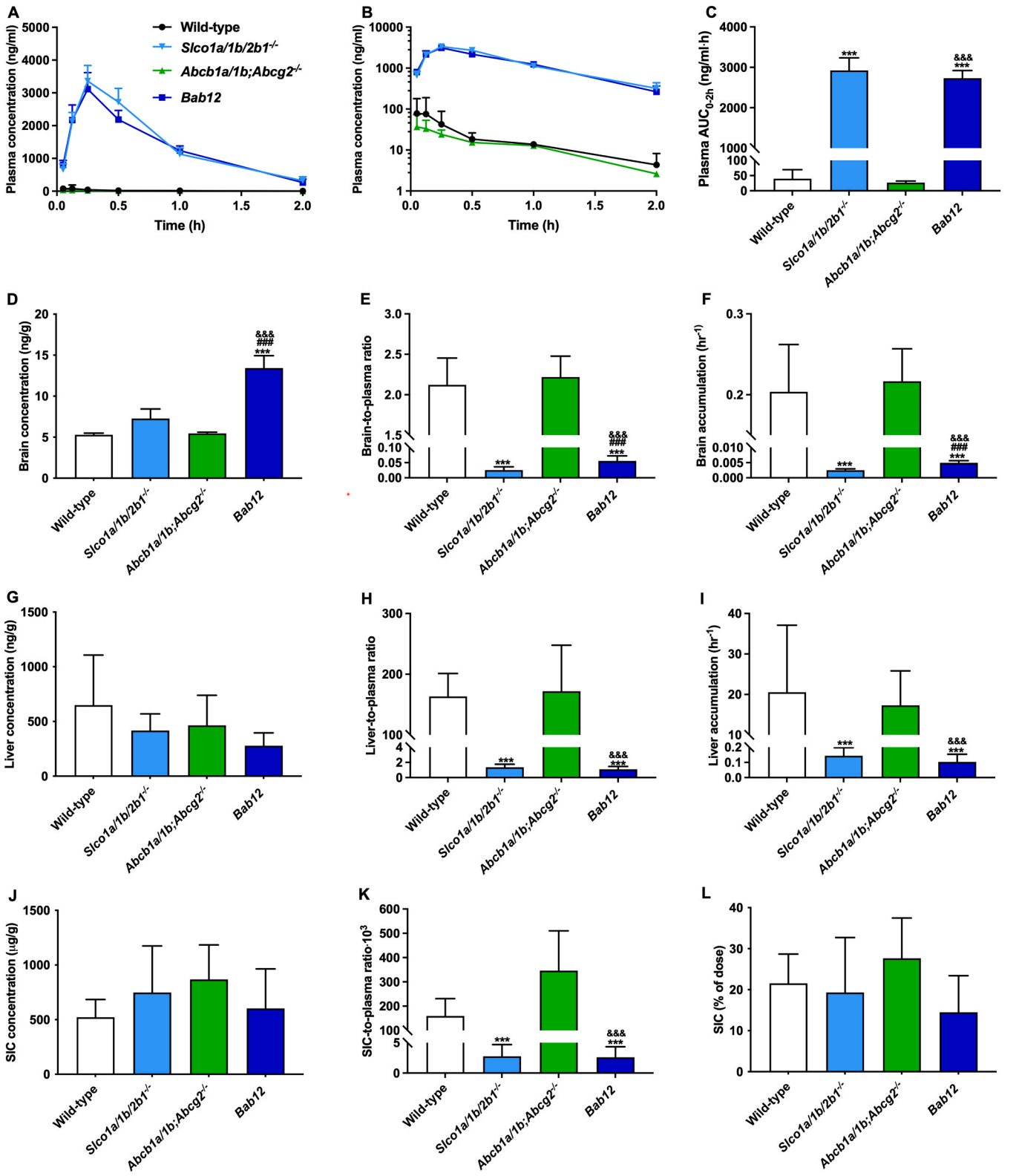

Fig. 5. Pravastatin plasma concentration-time curves (A) and semi-log plot of plasma concentration-time curves (B), plasma AUC_{0-2h} (C), brain/liver/SIC concentrations (D, G, J), brain-, liver-, SIC-to-plasma ratios (E, H, K), brain/liver accumulations (F, I), and SIC (% of dose) (L) in male wild-type, *Slco1a/1b/2b1*$^{-/-}$, *Abcb1a/1b;Abcg2*$^{-/-}$, and *Bab12* mice after oral administration of 10 mg/kg pravastatin. Data are presented as mean ± SD (n = 6). SIC, small intestinal content. SIC (% of dose), drug percentage of dose in SIC expressed as total pravastatin in SIC divided by total drug administered to the mouse. *, $P < 0.05$; **, $P < 0.01$; ***, $P < 0.001$ compared to wild-type mice. $^{\#}$, $P < 0.05$; $^{\#\#}$, $P < 0.01$; $^{\#\#\#}$, $P < 0.001$ comparing *Bab12* to *Slco1a/1b/2b1*$^{-/-}$ mice. $^{\&}$, $P < 0.05$; $^{\&\&}$, $P < 0.01$; $^{\&\&\&}$, $P < 0.001$ comparing *Bab12* to *Abcb1a/1b;Abcg2*$^{-/-}$ mice. Wild-type and *Slco1a/1b/2b1*$^{-/-}$ data were presented previously [25].

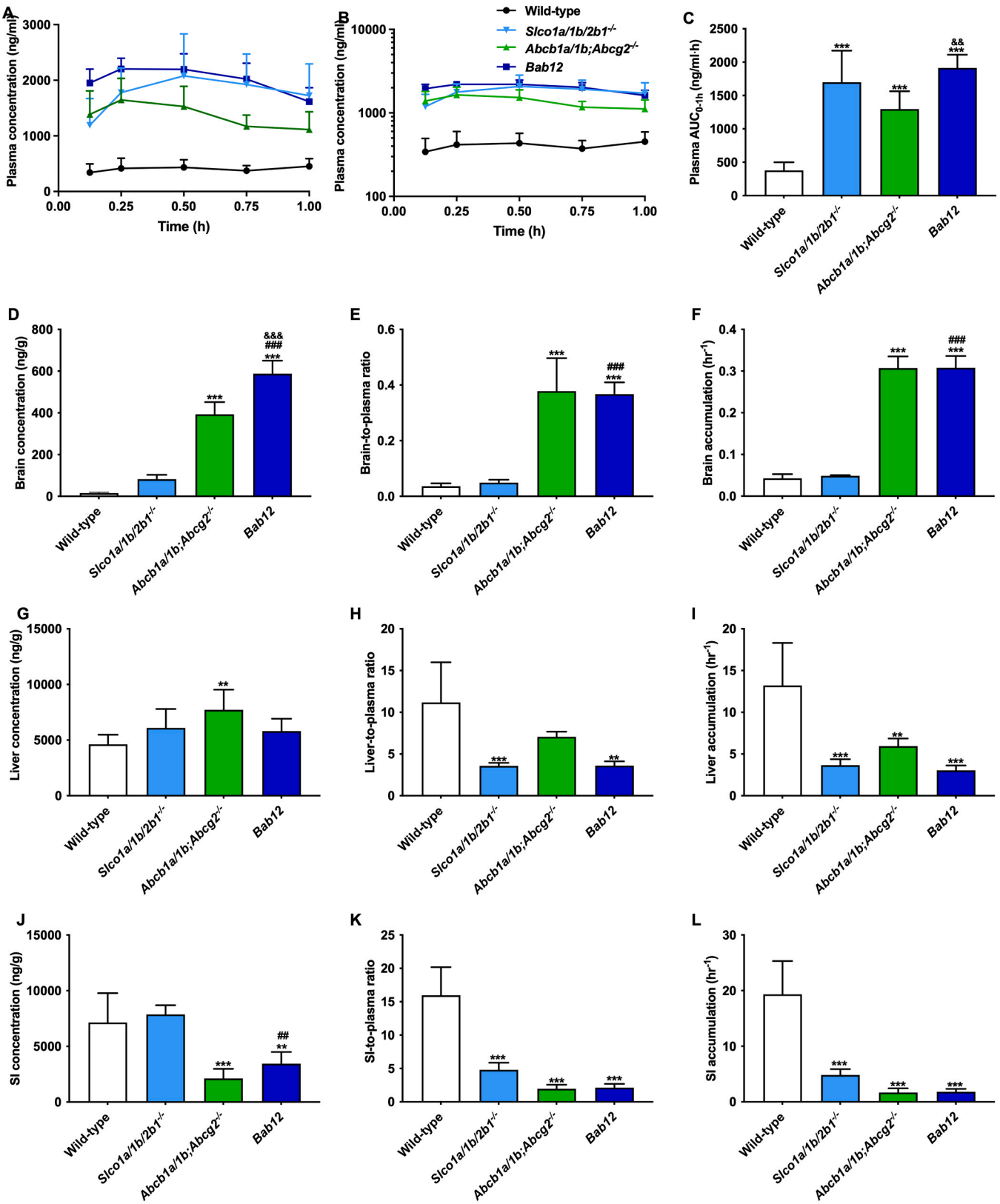

Fig. 6. Larotrectinib plasma concentration-time curves (A) and semi-log plot of plasma concentration-time curves (B), plasma AUC_{0-1h} (C), brain/liver/small intestinal tissue (SI) concentrations (D, G, J), brain-, liver-, SI-to-plasma ratios (E, H, K), and brain/liver/SI accumulations (F, I, L) in male wild-type (n = 7), *Slco1a/1b/2b1*$^{-/-}$ (n = 4), *Abcb1a/1b;Abcg2*$^{-/-}$ (n = 6), and *Bab12* (n = 6) mice after oral administration of 10 mg/kg larotrectinib. Data are presented as mean ± SD. *, $P < 0.05$; **, $P < 0.01$; ***, $P < 0.001$ compared to wild-type mice. $^{\#}$, $P < 0.05$; $^{\#\#}$, $P < 0.01$; $^{\#\#\#}$, $P < 0.001$ comparing *Bab12* to *Slco1a/1b/2b1*$^{-/-}$ mice. $^{\&}$, $P < 0.05$; $^{\&\&}$, $P < 0.01$; $^{\&\&\&}$, $P < 0.001$ comparing *Bab12* to *Abcb1a/1b;Abcg2*$^{-/-}$ mice. Wild-type and *Abcb1a/1b;Abcg2*$^{-/-}$ data were shown before [32].

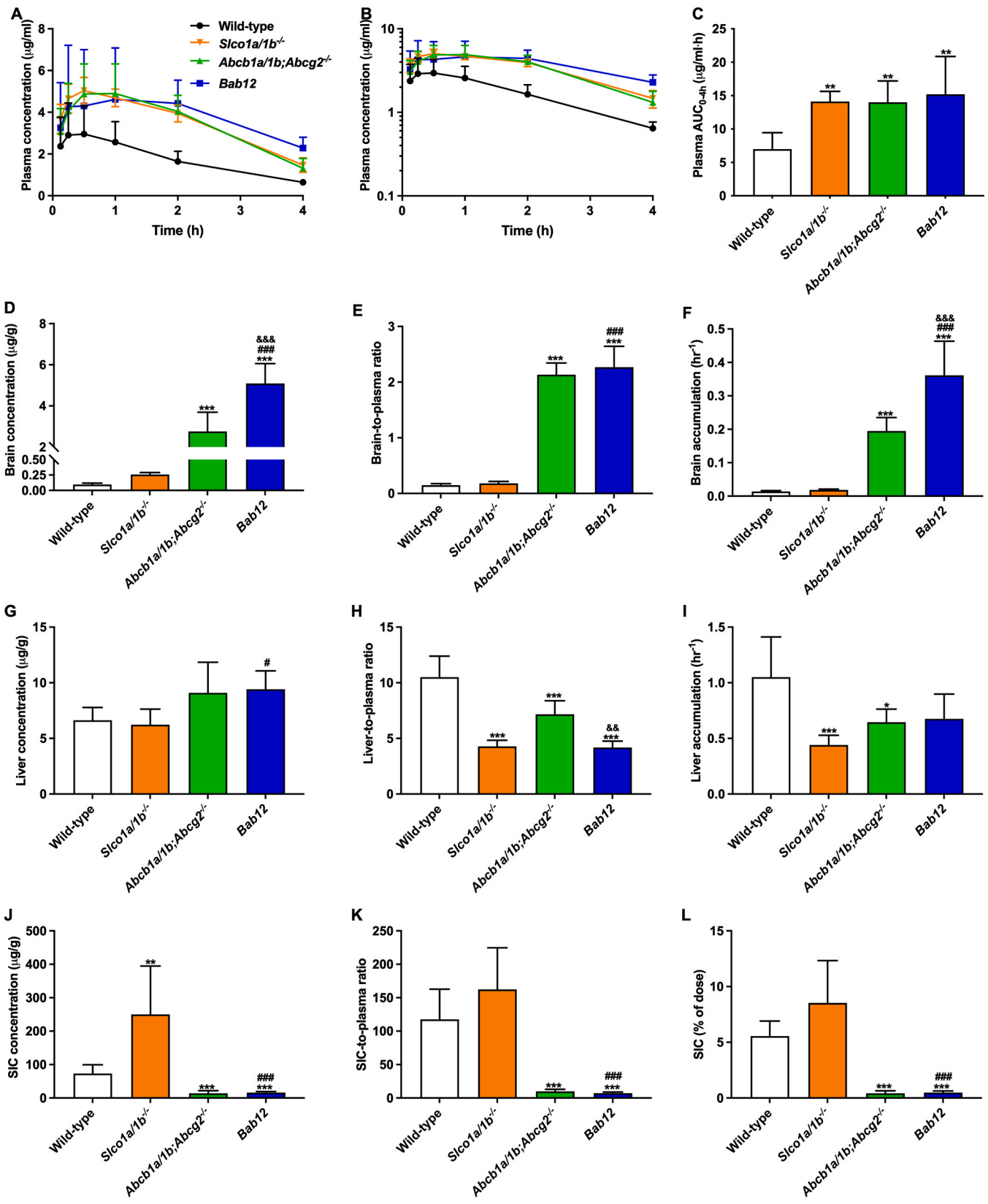

Fig. 7. Repotrectinib plasma concentration-time curves (A) and semi-log plot of plasma concentration-time curves (B), plasma AUC_{0-2h} (C), brain/liver/SIC concentrations (D, G, J), brain-, liver-, SIC-to-plasma ratios (E, H, K), brain/liver accumulations (F, I), and SIC (% of dose) (L) in male wild-type (n = 7), *Slco1a/1b*$^{-/-}$ (n = 6), *Abcb1a/1b;Abcg2*$^{-/-}$ (n = 6), and *Bab12* (n = 6) mice after oral administration of 10 mg/kg repotrectinib. Data are presented as mean ± SD. SIC, small intestinal content. SIC (% of dose), drug percentage of dose in SIC expressed as total repotrectinib in SIC divided by total drug administered to the mouse. *, $P < 0.05$; **, $P < 0.01$; ***, $P < 0.001$ compared to wild-type mice. $^{\#}$, $P < 0.05$; $^{\#\#}$, $P < 0.01$; $^{\#\#\#}$, $P < 0.001$ comparing *Bab12* to *Slco1a/1b*$^{-/-}$ mice. $^{\&}$, $P < 0.05$; $^{\&\&}$, $P < 0.01$; $^{\&\&\&}$, $P < 0.001$ comparing *Bab12* to *Abcb1a/1b;Abcg2*$^{-/-}$ mice. Wild-type, *Slco1a/1b*$^{-/-}$, and *Abcb1a/1b;Abcg2*$^{-/-}$ data were presented before [33].

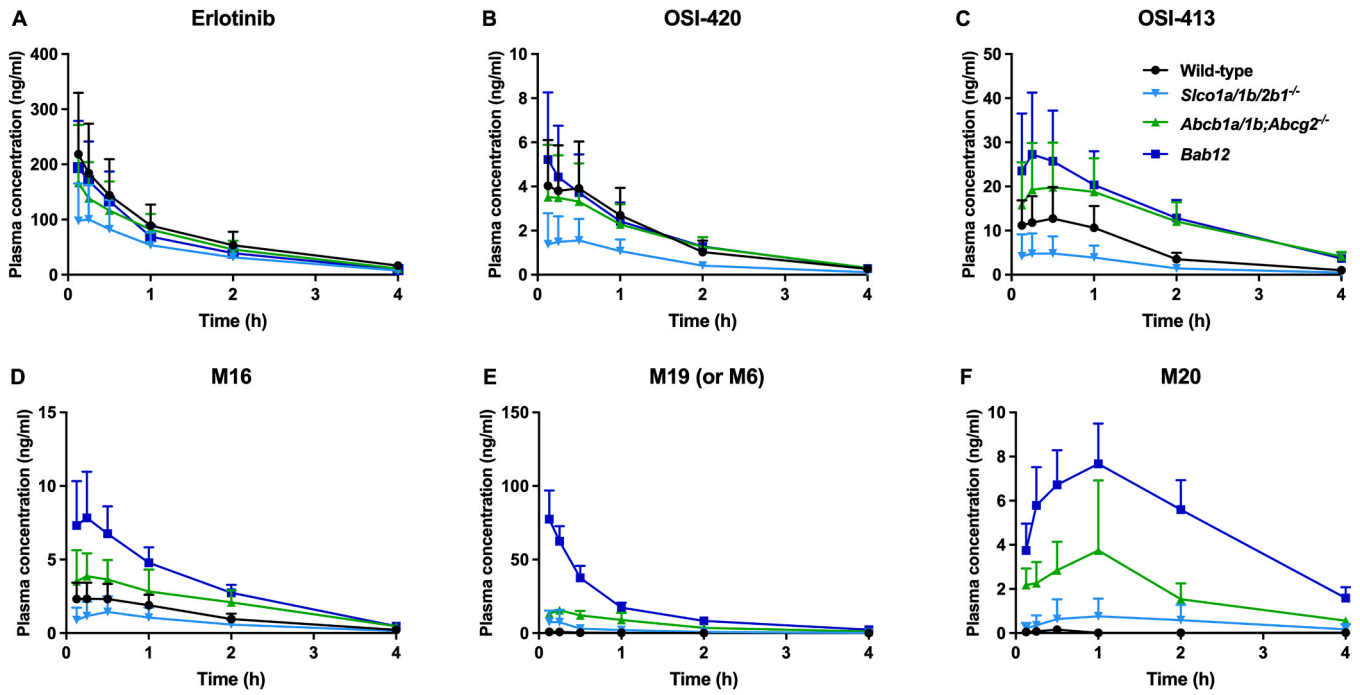

Fig. 8. The plasma concentration-time curves of erlotinib (A) and its metabolites (B-F) over 4 hours in male wild-type, *Slco1a/1b/2b1*$^{-/-}$, *Abcb1a/1b;Abcg2*$^{-/-}$, and *Bab12* mice after oral administration of 1 mg/kg erlotinib. Data are presented as mean ± SD (n = 6). The concentrations of erlotinib and OSI-420 were quantified and other concentrations were semi-quantified.

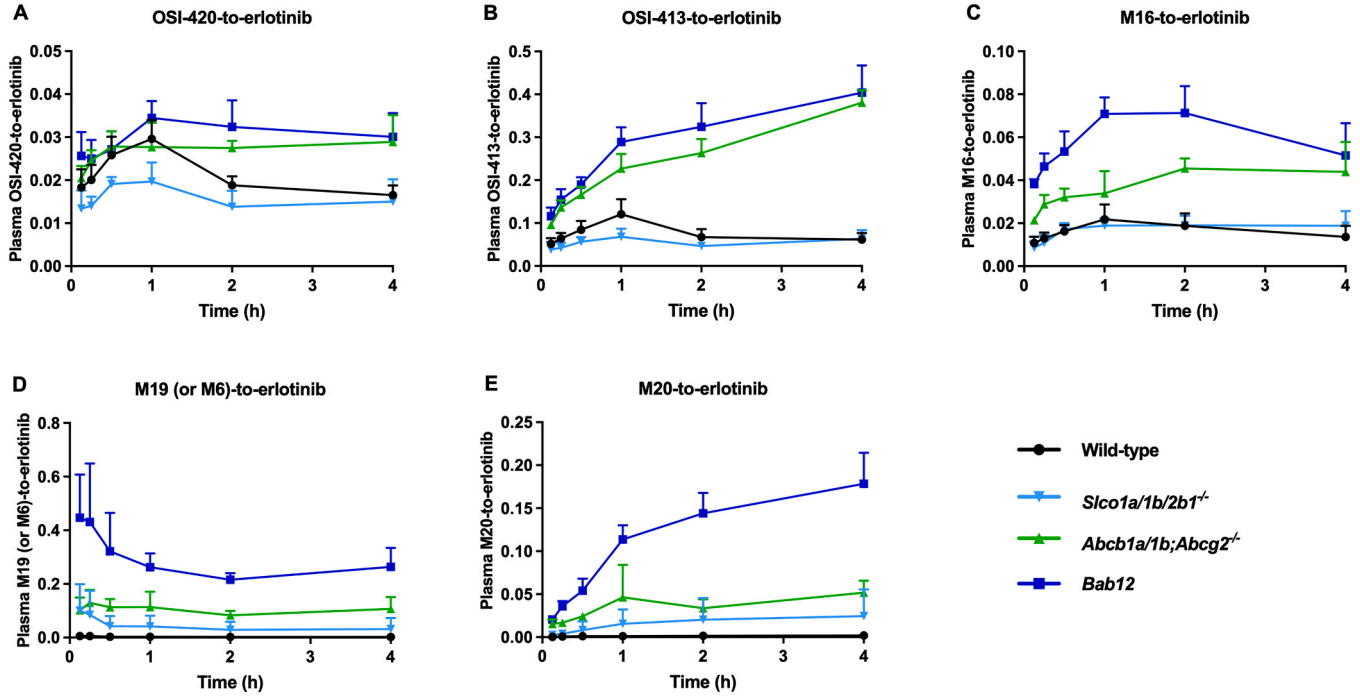

Fig. 9. Plasma concentration ratios of OSI-420 and erlotinib (A) and the plasma peak response area ratio of other metabolites and erlotinib (B-E) over 4 hours in male wild-type, *Slco1a/1b/2b1*$^{-/-}$, *Abcb1a/1b;Abcg2*$^{-/-}$, and *Bab12* mice after oral administration of 1 mg/kg erlotinib. Data are presented as mean ± SD (n = 6).

toxicological impact of these functionally complementary drug transporters. *Bab12* mice are viable and fertile, but they showed some abnormal phenotypes in their liver, spleen, and suborbital Harderian gland, possibly contributing to a slightly shorter life span. Moreover, we found that the plasma levels of BMG and BDG, but not UCB, were significantly higher in *Bab12* mice, both male and female, compared to *Slco1a/1b/2b1*$^{-/-}$ mice, suggesting that Abcb1a/1b and/or (more likely) Abcg2 contribute to endogenous conjugated bilirubin clearance. These data emphasize that these uptake and efflux transporters play an important role in the maintenance of physiological homeostasis.

Rosuvastatin, fexofenadine, fluvastatin, pravastatin, larotrectinib and repotrectinib were selected as candidate probe drugs to investigate the potential additive or counteracting pharmacological and toxicological roles of these transporters, because these compounds are substrates

of both uptake and efflux transporters. The main read-outs are summarized in Tables S9–S12. We found that the plasma exposures of rosuvastatin and fexofenadine were markedly increased in *Slco1a/1b/2b1*$^{-/-}$ and *Abcb1a/1b;Abcg2*$^{-/-}$ mice compared to wild-type mice, and then further substantially enhanced in *Bab12* mice, indicating an additive effect of the drug elimination functions of these uptake and efflux transporters. In contrast, significantly higher oral availability of fluvastatin and pravastatin was only observed in *Slco1a/1b/2b1*$^{-/-}$ and *Bab12* mice, with similar levels between the two strains, compared to wild-type mice, suggesting a dominant role of the uptake transporters for oral availability of these two drugs (Table S9). In addition, noticeable transport effects of on the one hand Slco1a/1b/2b1 and on the other hand Abcb1a/1b and Abcg2 in the BBB were observed for fluvastatin and pravastatin, respectively, when comparing *Bab12* mice with *Abcb1a/1b;Abcg2*$^{-/-}$ or *Slco1a/1b/2b1*$^{-/-}$ mice (Table S10). However, interpretation of the fluvastatin results was complicated by the widely different plasma exposure conditions. Surprisingly, although larotrectinib and repotrectinib plasma and tissue pharmacokinetics were markedly affected by the absence of either uptake transporters or efflux transporters, for these drugs no pronounced additional effects were observed for the combined transporter deficiencies. Furthermore, divergent behavior in plasma exposure of erlotinib and its metabolites was observed in *Bab12* mice.

We previously showed that both mouse Slco1a/1b and Slco2b1 transporters could contribute to endogenous bilirubin disposition [8,25]. Furthermore, Bockor et al. (2017) showed that while about 60% of *Ugt1*$^{-/-}$ mice survived after temporary phototherapy, all *Abcb1a/1b*$^{-/-}$*; Ugt1*$^{-/-}$ mice died before postnatal day 21, showing higher cerebellar levels of unconjugated bilirubin (UCB). This indicates that Abcb1 can play a critical role in the protection of the cerebellum from UCB toxicity during neonatal development, under extreme conditions [41]. Moreover, in *Abcg2*$^{-/-}$ mice, Vlaming et al. (2009) observed mildly increased plasma levels of UCB [42]. Therefore, UCB appears to be a substrate of these ABC transporters. However, we did not observe any changes in UCB plasma levels in *Abcb1a/1b;Abcg2*$^{-/-}$ mice compared to wild-type mice. Furthermore, whereas the concentrations of BMG and BDG were significantly further increased in *Bab12* compared to *Slco1a/1b/2b1*$^{-/-}$ mice, this was not the case for UCB. These data together suggest that Abcb1a/1b and/or Abcg2 can noticeably transport conjugated bilirubin, but perhaps only when its levels reach a certain threshold. Normally Abcc2 and Abcc3 play an important role in the disposition of conjugated bilirubin by hepatobiliary excretion into bile or direct efflux from liver into plasma, respectively [42,43]. Therefore, the impaired re-uptake of conjugated bilirubin from plasma into liver when Slco1a/1b/2b1 are absent resulted in highly elevated plasma levels. Perhaps through renal excretion Abcb1a/1b and/or Abcg2 in the proximal tubules of the kidney can then still modestly reduce the plasma levels of conjugated bilirubin. While for UCB, the Ugt1 enzyme is the most important clearance determinant, and the transporters appear to play only a minor or even negligible role in its clearance.

Statins are widely prescribed to lower low-density lipoprotein cholesterol levels to reduce cardiovascular morbidity and mortality. However, their therapy discontinuation and non-adherence remains a major concern, mostly due to the development of statin-associated muscle toxicity [44]. The risks of toxic myopathy are greatly increased by conditions that elevate blood statin levels, such as concomitant medications that interfere with statin metabolism or disposition via the CYP enzymes, glucuronidation, or excretion [45]. For example, statins are often prescribed to reduce the cardiovascular risks for transplant recipients, whose transplant immunosuppressant regimens often include cyclosporine. Cyclosporine inhibits CYP3A4-mediated statin metabolism and drug transporter mechanisms, among which CYP3A4 inhibition is thought to be the primary mechanism causing pharmacokinetic interactions. Thus, atorvastatin, simvastatin, lovastatin, and pitavastatin, all CYP3A substrates, should be avoided when patients are managed with cyclosporine. Rosuvastatin, fluvastatin and pravastatin, which mainly interact with cyclosporine through transporter inhibition mechanisms, are still recommended by the FDA for use in cyclosporine-treated patients, albeit at reduced doses [46]. Therefore, the interplay between Slco1a/1b/2b1 uptake transporters and Abcb1a/1b and Abcg2 efflux transporter was investigated using these three statins as candidate probes.

The systemic exposure of rosuvastatin was markedly increased in *Slco1a/1b/2b1*$^{-/-}$ (24.4-fold) and *Abcb1a/1b;Acbg2*$^{-/-}$ (2.4-fold) mice, and further dramatically increased more than 110-fold in *Bab12* mice compared to wild-type mice. This suggests that oral availability of rosuvastatin was modulated and controlled by the collaborative effects of Slco1a/1b/2b1, Abcb1a/1b, and Abcg2. However, such an additive effect between these uptake and efflux transporters was not observed in the plasma exposure of fluvastatin and pravastatin. For fluvastatin and pravastatin hardly any impact of the ABC transporters was observed on plasma exposure, while there was a strong impact of Slco1a/1b/2b1 (Figs. 4 and 5). For both compounds, only in brain penetration there was a noticeable limiting effect of the ABC transporters. The highly elevated plasma levels of rosuvastatin in the combined absence of Slco1a/1b/2b1, Abcb1a/1b, and Abcg2 transporters, but not of fluvastatin and pravastatin, may partially explain why rosuvastatin has the highest rates of reported side effects: the findings suggest a high sensitivity of rosuvastatin kinetics to changes in the activity of these transporters. In contrast, pravastatin and fluvastatin belong to the least myotoxic statin classes [45,47]. Indeed, DeGorter et al. (2013) found a marked, 45-fold interpatient variability in rosuvastatin plasma levels, especially at high doses, due to polymorphisms in the SLCO1B1 and ABCG2 drug transporters [37]. While in a randomized controlled trial in renal transplant patients taking cyclosporine (ALERT), fluvastatin 80 mg/d was well tolerated, with no differences compared to placebo in the incidence of myopathy [48]. In other words, the fact that rosuvastatin pharmacokinetics is affected by a number of different detoxifying systems that may vary in activity between patients and tend to act in an additive way will more likely result in inappropriate exposure levels.

Several studies have claimed to show that the mouse Oatp1a4 and Oatp2b1 transporters are expressed in endothelial cells at the BBB, where they might facilitate uptake of substrates into the brain [49,50]. Yet, previously we did not observe any significant contribution of these transporters to brain distribution of the substrates tested in Slco-deficient mice. Efflux transporters, such as ABCB1 and ACBG2 expressed at the luminal (apical) membrane of brain microvessel endothelial cells, actively pump the substrates out of the brain, which might overwhelm the uptake functions of OATPs. Conversely, OATP-mediated uptake (influx) may possibly also outcompete the ABC transporter-mediated efflux of some substrates. Interestingly, we may have observed instances of these two possible mechanisms in the present study (Table S10). Although the brain-to-plasma ratios of fluvastatin remained unaltered in *Slco1a/1b/2b1*$^{-/-}$ mice compared to wild-type mice, *Bab12* mice showed significantly reduced brain-to-plasma ratios compared to *Abcb1a/1b;Abcg2*$^{-/-}$ mice (Fig. 4E), which might suggest a net brain uptake function of one or more of the BBB Oatp proteins. However, the large differences in plasma exposure between these two strains may complicate straightforward analysis of these differences. While for pravastatin brain distribution, markedly higher brain-to-plasma ratios were observed in *Bab12* mice compared to *Slco1a/1b/2b1*$^{-/-}$ mice, whereas *Abcb1a/1b;Abcg2*$^{-/-}$ showed similar pravastatin brain accumulation as wild-type mice (Fig. 5E). For pravastatin there was little or no difference in plasma exposure between the compared strains, making an interpretation more reliable. These data could be in line with the hypothesized mechanisms above, namely that OATP1A/1B/2B1 transporters could mediate the uptake of fluvastatin into the brain and that Abcb1a/1b and/or Abcg2 transporters kept pravastatin out of brain, but that these functions could only be observed when the counteracting efflux and uptake transporters, respectively, were absent. Thus, *Bab12* mice together with the previously established *Slco1a/1b/2b1*$^{-/-}$ and *Abcb1a/1b;Abcg2*$^{-/-}$ mice would be a more sensitive

and useful set of mouse models to investigate the interplay of these transporters in the brain distribution of substrates.

In order to observe more clear vectorial transport of shared substrates for uptake and efflux transporters from the basal to the apical side compared with that in the opposite direction, double-transduced Madin-Darby canine kidney II (MDCK-II) cells expressing OATP1B1 in the basolateral membrane and ABCB1 or ABCG2 in the apical membrane have been established [51]. Using this model, Matsushima et al. (2005) found that there was a modest apically directed transport of pravastatin in both the double-transduced cell lines while no noticeable translocation of pravastatin was observed in single OATP1B1-, ABCB1- or ABCG2-expressing MDCK-II cells [51]. Whereas in our study, we did not find any obvious *in vivo* contribution of ABCB1 and/or ABCG2 to the modulation of pravastatin hepatobiliary excretion or systemic exposure. Probably, there are some other efflux system(s) *in vivo* playing a dominant role in mediating pravastatin biliary excretion, such as Abcc2, which has been found to be primarily responsible for this process in rats [52]. This may further suggest that the process of translocation of substrates by transporters in *in vitro* systems may not always properly reflect the extent to which a drug will be affected in an intact organism, as not all relevant factors (e.g., transporters) may be expressed *in vitro*. Often *in vivo* there will be many other factors involved, such as tissue distribution and interaction with other drug-handling systems not present in the *in vitro* model, as well as perhaps a limiting impact of blood flow.

Analogous to the mechanism of the double-transduced cell system, we may consider our newly generated *Bab12* mice as a control group (parental cell line without studied transporters): when the Slco1a/1b/2b1 transporters were introduced (as in the *Abcb1a/1b;Abcg2*$^{-/-}$ mice), hepatic uptake of substrates was facilitated, leading to reduced systemic exposure. In contrast, in the *Slco1a/1b/2b1*$^{-/-}$ mice, essentially presenting *Bab12* mice in which Abcb1a/1b and Abcg2 were introduced, these ABC transporters could mediate hepatobiliary excretion of absorbed substrates and directly efflux the substrates across the intestinal wall back to the intestinal lumen, speeding up the elimination of substrates and thus lowering their oral availability. In this view wild-type mice represent the 'double-transduced' system, where substrates were taken up into the liver and (perhaps) intestine by Slco1a/1b/2b1, and subsequently excreted into the intestinal lumen through biliary and intestinal excretion by Abcb1a/1b and Abcg2 (Tables S11 and S12). This tandem function of uptake and efflux transporters usually cooperatively accelerates the elimination of compounds. This explains why we observed dramatically reduced plasma exposure of rosuvastatin and fexofenadine in wild-type mice compared to *Bab12* mice, whereas 'single-transduced' systems (single knockout mice) showed relatively modest reductions compared to *Bab12* mice.

However, this tandem function and additive effect of transporters was not observed in the plasma exposure or tissue distribution of larotrectinib and repotrectinib, which have also been identified as good substrates of both the efflux and uptake transporters. We still do not fully understand the mechanism behind the missing additional impact of these transporters for some drugs, although saturation effects (of these transporters themselves, or of putative compensatory transporters or other detoxification systems) might play a role.

We further observed such additional and tandem functions of these transporters in the plasma exposure of some erlotinib metabolites (M16, M19 (or M6), M20), which showed dramatically higher plasma exposure in *Bab12* mice compared to the other three mouse strains (Figs. 8 and 9). Looking ahead for the application of this newly generated *Bab12* model, it may provide a useful and important model in drug discovery and clinical application, including safety and toxicity aspects. Although the interaction of statins with cyclosporine was quickly appreciated when rhabdomyolysis was first reported in cardiac transplant recipients, it took many years to understand the underlying mechanism. Furthermore, pralsetinib (Gavreto), a RET inhibitor recently approved for the treatment of metastatic RET fusion-positive NSCLC, inhibits ABCB1, ABCG2, OATP1B1 and OATP1B3 at therapeutic concentrations based on the instructions of the manufacturer [53]. From our present results using *Bab12* mice, it may suggest that patients treated with pralsetinib may have a higher risk of showing adverse effects when co-administered fexofenadine and especially rosuvastatin.

The expression of orthologs of these multidrug transporters is likely somewhat different between mice and humans, and thus the importance of relative transporter effects between these species could be different. Moreover, reduction and sometimes even complete loss of activity of some transporters due to genetic polymorphisms, such as single nucleotide polymorphisms (SNPs), have been identified and reported [19,54]. One can readily imagine that patients with reduced activity of OATP transporters may have dramatically elevated systemic exposure of substrates behaving like rosuvastatin and fexofenadine when they are receiving concomitant inhibitor(s) of the ABC transporters, and *vice versa*. Application of the *Bab12* mouse model may provide an adequate and useful approach to identify and explain the adverse effects due to such transporter-mediated drug-drug interactions combined with genetic polymorphisms, thus potentially reducing the toxicity of drugs in the clinic. A main advantage of the *Bab12* mouse model and its controls is that it allows a relatively specific analysis of the contribution of each of the constituent transporters. Analysis of such *in vivo* functions by using relatively specific inhibitors is nearly always potentially compromised. This is because it is impossible to guarantee that these inhibitors do not affect any other relevant *in vivo* detoxifying systems, some of which may not even have been functionally linked to the research compound in question.

5. Conclusions

The present study provides new insights into some physiological functions by showing the interplay between the Slco1a/1b/2b1, Abcb1a/1b, and Abcg2 transporters affecting bilirubin disposition, together with Abcc2 and Abcc3 (the latter based on preceding studies [8,42]). Moreover, we demonstrated here additional effects and tandem functions of these transporters in modulating the plasma exposure and tissue distribution of various drug substrates. The *Bab12* mice and comparison with the constituent strains will further help to identify rate-limiting factors for transporter-mediated pharmacokinetics and drug-drug interactions. This study thus establishes the validity and usefulness of the *Bab12* mouse model in studying the pharmacological and toxicological impact of transporters on substrates, which may be used to optimize the clinical application of drugs.

Funding statement

This work was funded in part by China Scholarship Council (No. 201606220081; No. 201506240107), National Natural Science Foundation of China (No. 82304554), and DiacetylM BV.

CRediT authorship contribution statement

Olaf van Tellingen: Writing – review & editing, Investigation, Data curation. **Dirk R. de Waart:** Writing – review & editing, Investigation, Data curation. **Margarida L. F. Martins:** Writing – review & editing, Investigation. **Yaogeng Wang:** Writing – review & editing, Investigation. **Rolf W. Sparidans:** Writing – review & editing, Investigation, Data curation. **Alfred H. Schinkel:** Writing – review & editing, Supervision, Project administration, Conceptualization. **Wenlong Li:** Writing – original draft, Methodology, Investigation, Formal analysis, Data curation, Conceptualization. **Jos H. Beijnen:** Writing – review & editing, Supervision. **Els Wagenaar:** Methodology, Investigation, Data curation. **Stéphanie van Hoppe:** Writing – review & editing. **Maria C. Lebre:** Writing – review & editing, Resources. **Ji-Ying Song:** Writing – review & editing, Investigation.

Declaration of Competing Interest

The authors declare the following financial interests/personal relationships which may be considered as potential competing interests: Wenlong Li reports financial support was provided by China Scholarship Council and National Natural Science Foundation of China. Yaogeng Wang reports financial support was provided by China Scholarship Council. Margarida Martins reports financial support was provided by DiacetylM BV. Alfred Schinkel reports a relationship with Taconic Biosciences Inc that includes: funding grants.

Data availability

Data will be made available on request.

Acknowledgements

We gratefully acknowledge the support from the Genomic Core Facility of the Netherlands Cancer Institute in performing RNA sequencing analysis. We also thank Bart van Wijnen of the Clinical Chemistry lab at the Netherlands Cancer Institute for the clinical chemistry measurements of mouse plasma. We are further grateful for the support from the animal facility of the Netherlands Cancer Institute.

Appendix A. Supporting information

Supplementary data associated with this article can be found in the online version at doi:10.1016/j.biopha.2024.116644.

References

[1] K.M. Giacomini, S.M. Huang, D.J. Tweedie, L.Z. Benet, K.L.R. Brouwer, X. Chu, et al., Membrane transporters in drug development, Nat. Rev. Drug Discov. 9 (3) (2010) 215–236.
[2] X. Chu, G.H. Chan, R. Evers, Identification of Endogenous Biomarkers to Predict the Propensity of Drug Candidates to Cause Hepatic or Renal Transporter-Mediated Drug-Drug Interactions, J. Pharm. Sci. 106 (9) (2017) 2357–2367.
[3] C.C. Paulusma, M. Kool, P.J. Bosma, G.L. Scheffer, F. ter Borg, R.J. Scheper, et al., A mutation in the human canalicular multispecific organic anion transporter gene causes the Dubin-Johnson syndrome, Hepatol. Balt. Md 25 (6) (1997) 1539–1542.
[4] T. Kamisako, Y. Kobayashi, K. Takeuchi, T. Ishihara, K. Higuchi, Y. Tanaka, et al., Recent advances in bilirubin metabolism research: the molecular mechanism of hepatocyte bilirubin transport and its clinical relevance, J. Gastroenterol. 35 (9) (2000) 659–664.
[5] F. Quazi, R.S. Molday, Lipid transport by mammalian ABC proteins, Essays Biochem 50 (1) (2011) 265–290.
[6] M. Roth, A. Obaidat, B. Hagenbuch, OATPs, OATs and OCTs: the organic anion and cation transporters of the SLCO and SLC22A gene superfamilies, Br. J. Pharm. 165 (5) (2012) 1260–1287.
[7] A.H. Schinkel, J.W. Jonker, Mammalian drug efflux transporters of the ATP binding cassette (ABC) family: an overview, Adv. Drug Deliv. Rev. 55 (1) (2003) 3–29.
[8] E. van de Steeg, E. Wagenaar, C.M.M. van der Kruijssen, J.E.C. Burggraaff, D.R. de Waart, R.P.J.O. Elferink, et al., Organic anion transporting polypeptide 1a/1b–knockout mice provide insights into hepatic handling of bilirubin, bile acids, and drugs, J. Clin. Invest 120 (8) (2010) 2942–2952.
[9] S.J. McFeely, L. Wu, T.K. Ritchie, J. Unadkat, Organic anion transporting polypeptide 2B1 - More than a glass-full of drug interactions, Pharm. Ther. 196 (2019) 204–215.
[10] S. Choudhuri, C.D. Klaassen, Structure, function, expression, genomic organization, and single nucleotide polymorphisms of human ABCB1 (MDR1), ABCC (MRP), and ABCG2 (BCRP) efflux transporters, Int J. Toxicol. 25 (4) (2006) 231–259.
[11] R.R. Begicevic, M. Falasca, ABC Transporters in Cancer Stem Cells: Beyond Chemoresistance, Int J. Mol. Sci. 18 (11) (2017) 2362.
[12] V. Buxhofer-Ausch, L. Secky, K. Wlcek, M. Svoboda, V. Kounnis, E. Briasoulis, et al., Tumor-specific expression of organic anion-transporting polypeptides: transporters as novel targets for cancer therapy, J. Drug Deliv. 2013 (2013) 863539.
[13] K.M. Giacomini, Y. Sugiyama, Membrane Transporters and Drug Response, in: L. L. Brunton, R. Hilal-Dandan, B.C. Knollmann (Eds.), Goodman & Gilman's: The Pharmacological Basis of Therapeutics, 13e [Internet]., McGraw-Hill Education, New York, NY, 2017. ⟨accessmedicine.mhmedical.com/content.aspx?aid=1162533244⟩ [cited 2023 Jul 9]. Available from:.
[14] A.T. Nies, M. Schwab, D. Keppler, Interplay of conjugating enzymes with OATP uptake transporters and ABCC/MRP efflux pumps in the elimination of drugs, Expert Opin. Drug Metab. Toxicol. 4 (5) (2008) 545–568.
[15] P.R. Criado, R.F.J. Criado, C.W. Maruta, C. Machado Filho, d'Apparecida. Histamine, histamine receptors and antihistamines: new concepts, Bras. Dermatol. 85 (2) (2010) 195–210.
[16] S.N. de Wildt, G.L. Kearns, J.S. Leeder, J.N. van den Anker, Cytochrome P450 3A: ontogeny and drug disposition, Clin. Pharm. 37 (6) (1999) 485–505.
[17] A.E. van Herwaarden, R.A.B. van Waterschoot, A.H. Schinkel, How important is intestinal cytochrome P450 3A metabolism? Trends Pharm. Sci. 30 (5) (2009) 223–227.
[18] S. Chen, N. Sutiman, C.Z. Zhang, Y. Yu, S. Lam, C.C. Khor, et al., Pharmacogenetics of irinotecan, doxorubicin and docetaxel transporters in Asian and Caucasian cancer patients: a comparative review, Drug Metab. Rev. 48 (4) (2016) 502–540.
[19] J.J.G. Marin, M.A. Serrano, M.J. Monte, A. Sanchez-Martin, A.G. Temprano, O. Briz, et al., Role of Genetic Variations in the Hepatic Handling of Drugs, Int J. Mol. Sci. 21 (8) (2020) 2884.
[20] N. Izat, S. Sahin, Hepatic transporter-mediated pharmacokinetic drug-drug interactions: Recent studies and regulatory recommendations, Biopharm. Drug Dispos. 42 (2–3) (2021) 45–77.
[21] L. Zhang, Y.D. Zhang, J.M. Strong, K.S. Reynolds, S.M. Huang, A regulatory viewpoint on transporter-based drug interactions, Xenobiotica Fate Foreign Compd. Biol. Syst. 38 (7–8) (2008) 709–724.
[22] R.H. Ho, L. Choi, W. Lee, G. Mayo, U.I. Schwarz, R.G. Tirona, et al., Effect of drug transporter genotypes on pravastatin disposition in European- and African-American participants, Pharm. Genom. 17 (8) (2007) 647–656.
[23] M. Uchida, Y. Tajima, M. Kakuni, Y. Kageyama, T. Okada, E. Sakurada, et al., Organic Anion–Transporting Polypeptide (OATP)–Mediated Drug-Drug Interaction Study between Rosuvastatin and Cyclosporine A in Chimeric Mice with Humanized Liver, Drug Metab. Dispos. 46 (1) (2018) 11–19.
[24] D. Wang, Current Research Method in Transporter Study, Adv. Exp. Med Biol. 1141 (2019) 203–240.
[25] W. Li, D. Iusuf, R.W. Sparidans, E. Wagenaar, Y. Wang, D.R. de Waart, et al., Organic anion-transporting polypeptide 2B1 knockout and humanized mice; insights into the handling of bilirubin and drugs, Pharm. Res 190 (2023) 106724.
[26] W. Spivak, M.C. Carey, Reverse-phase h.p.l.c. separation, quantification and preparation of bilirubin and its conjugates from native bile. Quantitative analysis of the intact tetrapyrroles based on h.p.l.c. of their ethyl anthranilate azo derivatives, Biochem J. 225 (3) (1985) 787–805.
[27] R.W. Sparidans, D. Iusuf, A.H. Schinkel, J.H.M. Schellens, J.H. Beijnen, Liquid chromatography-tandem mass spectrometric assay for pravastatin and two isomeric metabolites in mouse plasma and tissue homogenates, J. Chromatogr. B Anal. Technol. Biomed. Life Sci. 878 (28) (2010) 2751–2759.
[28] R.W. Sparidans, Y. Wang, A.H. Schinkel, J.H.M. Schellens, J.H. Beijnen, Quantitative bioanalytical assay for the tropomyosin receptor kinase inhibitor larotrectinib in mouse plasma and tissue homogenates using liquid chromatography-tandem mass spectrometry, J. Chromatogr. B Anal. Technol. Biomed. Life Sci. 1102–1103 (2018) 167–172.
[29] W. Li, N. Perpinioti, A.H. Schinkel, J.H. Beijnen, R.W. Sparidans, Bioanalytical assay for the new-generation ROS1/TRK/ALK inhibitor repotrectinib in mouse plasma and tissue homogenate using liquid chromatography-tandem mass spectrometry, J. Chromatogr. B 1144 (2020) 122098.
[30] J.J.M. Rood, J.S. Toraño, V.J. Somovilla, J.H. Beijnen, R.W. Sparidans, Bioanalysis of erlotinib, its O-demethylated metabolites OSI-413 and OSI-420, and other metabolites by liquid chromatography-tandem mass spectrometry with additional ion mobility identification, J. Chromatogr. B Anal. Technol. Biomed. Life Sci. 1166 (2021) 122554.
[31] Y. Zhang, M. Huo, J. Zhou, S. Xie, PKSolver: An add-in program for pharmacokinetic and pharmacodynamic data analysis in Microsoft Excel, Comput. Methods Prog. Biomed. 99 (3) (2010) 306–314.
[32] Y. Wang, R.W. Sparidans, W. Li, M.C. Lebre, J.H. Beijnen, A.H. Schinkel, OATP1A/1B, CYP3A, ABCB1, and ABCG2 limit oral availability of the NTRK inhibitor larotrectinib, while ABCB1 and ABCG2 also restrict its brain accumulation, Br. J. Pharm. 177 (13) (2020) 3060–3074.
[33] W. Li, R.W. Sparidans, M.C. Lebre, J.H. Beijnen, A.H. Schinkel, ABCB1 and ABCG2 Control Brain Accumulation and Intestinal Disposition of the Novel ROS1/TRK/ALK Inhibitor Repotrectinib, While OATP1A/1B, ABCG2, and CYP3A Limit Its Oral Availability, Pharmaceutics 13 (11) (2021) 1761.
[34] J.W. Jonker, S. Musters, M.L.H. Vlaming, T. Plösch, K.E.R. Gooijert, M. J. Hillebrand, et al., Breast cancer resistance protein (Bcrp1/Abcg2) is expressed in the harderian gland and mediates transport of conjugated protoporphyrin IX, Am. J. Physiol. Cell Physiol. 292 (6) (2007) C2204–C2212.
[35] S. Agarwal, Y. Uchida, R.K. Mittapalli, R. Sane, T. Terasaki, W.F. Elmquist, Quantitative proteomics of transporter expression in brain capillary endothelial cells isolated from P-glycoprotein (P-gp), breast cancer resistance protein (Bcrp), and P-gp/Bcrp knockout mice, Drug Metab. Dispos. 40 (6) (2012) 1164–1169.
[36] C.M. White, A review of the pharmacologic and pharmacokinetic aspects of rosuvastatin, J. Clin. Pharm. 42 (9) (2002) 963–970.
[37] M.K. DeGorter, R.G. Tirona, U.I. Schwarz, Y.H. Choi, G.K. Dresser, N. Suskin, et al., Clinical and pharmacogenetic predictors of circulating atorvastatin and rosuvastatin concentrations in routine clinical care, Circ. Cardiovasc Genet 6 (4) (2013) 400–408.
[38] H. Tahara, H. Kusuhara, E. Fuse, Y. Sugiyama, P-glycoprotein plays a major role in the efflux of fexofenadine in the small intestine and blood-brain barrier, but only a limited role in its biliary excretion, Drug Metab. Dispos. Biol. Fate Chem. 33 (7) (2005) 963–968.
[39] T. Vanhove, T. Bouillon, H. de Loor, P. Annaert, D. Kuypers, Fexofenadine, a Putative In Vivo P-glycoprotein Probe, Fails to Predict Clearance of the Substrate Tacrolimus in Renal Recipients, Clin. Pharm. Ther. 102 (6) (2017) 989–996.

[40] T. Karibe, R. Hagihara-Nakagomi, K. Abe, T. Imaoka, T. Mikkaichi, S. Yasuda, et al., Evaluation of the usefulness of breast cancer resistance protein (BCRP) knockout mice and BCRP inhibitor-treated monkeys to estimate the clinical impact of BCRP modulation on the pharmacokinetics of BCRP substrates, Pharm. Res 32 (5) (2015) 1634–1647.
[41] L. Bockor, G. Bortolussi, S. Vodret, A. Iaconcig, J. Jašprová, J. Zelenka, et al., Modulation of bilirubin neurotoxicity by the Abcb1 transporter in the Ugt1-/- lethal mouse model of neonatal hyperbilirubinemia, Hum. Mol. Genet. 26 (1) (2017) 145–157.
[42] M.L.H. Vlaming, Z. Pala, A. van Esch, E. Wagenaar, D.R. de Waart, K. van de Wetering, et al., Functionally overlapping roles of Abcg2 (Bcrp1) and Abcc2 (Mrp2) in the elimination of methotrexate and its main toxic metabolite 7-hydroxymethotrexate in vivo, Clin. Cancer Res J. Am. Assoc. Cancer Res 15 (9) (2009) 3084–3093.
[43] E. van de Steeg, V. Stránecký, H. Hartmannová, L. Nosková, M. Hřebíček, E. Wagenaar, et al., Complete OATP1B1 and OATP1B3 deficiency causes human Rotor syndrome by interrupting conjugated bilirubin reuptake into the liver, J. Clin. Invest 122 (2) (2012) 519–528.
[44] C.B. Newman, D. Preiss, J.A. Tobert, T.A. Jacobson, R.L. Page, L.B. Goldstein, et al., Statin Safety and Associated Adverse Events: A Scientific Statement From the American Heart Association, Arterioscler. Thromb. Vasc. Biol. 39 (2) (2019) e38–e81.
[45] D.M. Muntean, P.D. Thompson, A.L. Catapano, M. Stasiolek, J. Fabis, P. Muntner, et al., Statin-associated myopathy and the quest for biomarkers: can we effectively predict statin-associated muscle symptoms? Drug Discov. Today 22 (1) (2017) 85–96.
[46] K.A. Kellick, M. Bottorff, P.P. Toth, The National Lipid Association's Safety Task Force null. A clinician's guide to statin drug-drug interactions, J. Clin. Lipido 8 (3 Suppl) (2014) S30–S46.
[47] S.M. Wolfe, Should rosuvastatin be withdrawn from the market? Lancet 364 (9445) (2004) 1578–1579.
[48] H. Holdaas, B. Fellström, A.G. Jardine, I. Holme, G. Nyberg, P. Fauchald, et al., Effect of fluvastatin on cardiac outcomes in renal transplant recipients: a multicentre, randomised, placebo-controlled trial, Lancet Lond. Engl. 361 (9374) (2003) 2024–2031.
[49] A. Ose, H. Kusuhara, C. Endo, K. Tohyama, M. Miyajima, S. Kitamura, et al., Functional characterization of mouse organic anion transporting peptide 1a4 in the uptake and efflux of drugs across the blood-brain barrier, Drug Metab. Dispos. Biol. Fate Chem. 38 (1) (2010) 168–176.
[50] Z.Z. Yang, L. Li, L. Wang, M.C. Xu, S. An, C. Jiang, et al., siRNA capsulated brain-targeted nanoparticles specifically knock down OATP2B1 in mice: a mechanism for acute morphine tolerance suppression, Sci. Rep. 6 (2016) 33338.
[51] S. Matsushima, K. Maeda, C. Kondo, M. Hirano, M. Sasaki, H. Suzuki, et al., Identification of the hepatic efflux transporters of organic anions using double-transfected Madin-Darby canine kidney II cells expressing human organic anion-transporting polypeptide 1B1 (OATP1B1)/multidrug resistance-associated protein 2, OATP1B1/multidrug resistance 1, and OATP1B1/breast cancer resistance protein, J. Pharm. Exp. Ther. 314 (3) (2005) 1059–1067.
[52] M. Yamazaki, S. Akiyama, K. Ni'inuma, R. Nishigaki, Y. Sugiyama, Biliary excretion of pravastatin in rats: contribution of the excretion pathway mediated by canalicular multispecific organic anion transporter, Drug Metab. Dispos. Biol. Fate Chem. 25 (10) (1997) 1123–1129.
[53] K.M. Wright, FDA Approves Pralsetinib for Treatment of Adults With Metastatic RET Fusion-Positive NSCLC, Oncol. Williston Park N. 34 (10) (2020). :406-406; 431.
[54] E. Baudou, A. Lespine, G. Durrieu, F. André, P. Gandia, C. Durand, et al., Serious Ivermectin Toxicity and Human ABCB1 Nonsense Mutations, N. Engl. J. Med 383 (8) (2020) 787–789.